

# SYNAPTIC VESICLE EXOCYTOSIS CAPTURED BY QUICK FREEZING AND CORRELATED WITH QUANTAL TRANSMITTER RELEASE

J. E. HEUSER, T. S. REESE, M. J. DENNIS, Y. JAN, L. JAN,  
and L. EVANS

From the Department of Physiology, University of California, School of Medicine, San Francisco, California 94143, and the Section on Functional Neuroanatomy, Laboratory of Neuropathology and Neuroanatomical Sciences, National Institute of Neurological and Communicative Disorders and Stroke, National Institutes of Health, Bethesda, Maryland 20014. Drs. Jan's and Jan's present address is the Department of Neurobiology, Harvard Medical School, Boston, Mass 02115.

## ABSTRACT

We describe the design and operation of a machine that freezes biological tissues by contact with a cold metal block, which incorporates a timing circuit that stimulates frog neuromuscular junctions in the last few milliseconds before they are frozen. We show freeze-fracture replicas of nerve terminals frozen during transmitter discharge, which display synaptic vesicles caught in the act of exocytosis. We use 4-aminopyridine (4-AP) to increase the number of transmitter quanta discharged with each nerve impulse, and show that the number of exocytotic vesicles caught by quick-freezing increases commensurately, indicating that one vesicle undergoes exocytosis for each quantum that is discharged. We perform statistical analyses on the spatial distribution of synaptic vesicle discharge sites along the "active zones" that mark the secretory regions of these nerves, and show that individual vesicles fuse with the plasma membrane independent of one another, as expected from physiological demonstrations that quanta are discharged independently. Thus, the utility of quick-freezing as a technique to capture biological processes as evanescent as synaptic transmission has been established. An appendix describes a new capacitance method to measure freezing rates, which shows that the "temporal resolution" of our quick-freezing technique is 2 ms or better.

**KEY WORDS** synaptic vesicles · transmitter quanta · exocytosis · neurosecretion · neuromuscular junction · quick freezing

The hypothesis that nerve terminals discharge transmitter by exocytosis from synaptic vesicles has suffered, since its conception by del Castillo and Katz (16), from a lack of solid experimental evidence. Electron microscopy has failed to provide convincing views of synaptic vesicle exocytosis (5, 45), and the changes in structure of vesicles

and presynaptic membranes brought on by nerve stimulation have remained the subject of controversy (4, 10, 26, 46). Biochemical fractionation studies, which first demonstrated that synaptic vesicles contain a rich stock of neurotransmitters (57, 58), have not shown convincingly that transmitters are secreted from within synaptic vesicles, as opposed to secretion from an intermediate pool of transmitter dissolved in the axoplasm (19, 40, 60, 61). The strongest evidence to date has been that proteins and other contents of the vesicles are

discharged along with the neurotransmitter (cf. reference 38 for complete references).

In previous papers (25, 27), we presented electron microscope views of the presynaptic membrane, mainly from freeze-fracture preparations, which revealed what we thought were synaptic vesicles caught in the act of exocytosis by aldehyde fixation. We showed that "pockets" are plentiful in the presynaptic membrane only when nerves are fixed during stimulation and are absent when nerves are fixed at rest. Couteaux first observed such plasmalemmal pockets, and he, too thought they were synaptic vesicles in exocytosis (12). He illustrated such pockets occurring in restricted domains on the presynaptic membrane, which he named the "active zones" of the synapse.

One problem in accepting the electron micrographs of stimulated nerves as morphological proof of vesicle release is that the static images in fixed tissues might not be vesicles in the process of discharge (in exocytosis) but rather vesicles in the process of formation, or endocytosis. Our earlier studies of horseradish peroxidase uptake (26) indicated to us that endocytosis was very rare at the active zones, but this result was not universally accepted (10). Also, our previous studies had the serious shortcoming of failing to correlate the abundance of the plasmalemmal pockets with the rate of transmitter secretion recorded at the moment of fixation. Instead, the abundance of these presynaptic membrane perturbations depended on the chemical composition and the strength of the aldehyde fixative applied (27). We were forced to conclude that chemical fixation was too slow to capture definitively the rapid structural changes that accompany synaptic transmission.

To avoid the use of chemical fixation, we turned to quick-freezing, assuming that such physical fixation would arrest structural changes more rapidly and thus provide a more accurate view of presynaptic events at the time of transmitter release. We developed a machine to freeze tissues quickly, based on earlier designs of Van Harreveld (18, 20, 51, 52), and we learned to freeze-fracture frog muscles that had been frozen with this machine. At first, however, we could not obtain any images of synaptic vesicle exocytosis, nothing like the images that by now are commonly seen in chemically fixed nerve terminals (28). In the present report, we illustrate that this puzzling result has finally been explained by the response obtained by stimulating frog muscles in the presence of 4-aminopyridine (4-AP), which augments

evoked transmitter release from the frog neuromuscular junction by up to two orders of magnitude. With such enhanced transmitter release, plasmalemmal pockets like the ones we ascribed to synaptic vesicle exocytosis in fixed tissues turn out to be abundant also on nerve terminals quick-frozen after a single nerve stimulus. We have then gone on to show that these structures appear at virtually the same time that transmitter release occurs, and that they are nearly as abundant as the number of quanta that are released in the various doses of 4-AP. We have also examined the spatial distribution of these presumed exocytic vesicles, and find that they appear independent of one another. The results of our work agree with the hypothesis that each vesicle discharge releases an independent quantum of transmitter.

## MATERIALS AND METHODS

Cutaneous pectoris muscles were dissected from the smallest *Rana pipiens* we could obtain from Lake Champlain Frog Farm, our most consistent supplier of healthy specimens. (They designate such animals as one inch body length.) Both muscles, together with their motor nerves intact for 1 cm or more, were taken from each pithed animal. Each nerve-muscle preparation was mounted in a separate 5-ml Sylgard-bottomed Petri dish (Dow Corning Corp., Midland, Mich.) and refrigerated in frog Ringer's containing 116 mM sodium chloride, 2 mM potassium chloride, 2 mM calcium chloride, 0.5 mM sodium phosphate, and 5 mM HEPES buffer, with 5% glucose added. Muscles were used 1–6 h later, depending on whether they were dissected near the beginning or the end of the day's experiments.

### Quick Freezing

Each muscle was removed in sequence from the refrigerator and soaked at room temperature in Ringer's containing the drugs 4-AP (Sigma Chemical Co., St. Louis, Mo.) and curare at the various strengths described in Results. The calcium concentration of the Ringer's was simultaneously raised to 10 mM to prevent spontaneous or repetitive nerve firing (see Results). This soak lasted 15–60 min, after which the muscle was mounted in the freezing machine, stimulated, and frozen.

Mounting in the freezing machine (Fig. 1) was a potentially damaging step, because the muscle had to be lifted out of the Petri dish and draped over an 800- $\mu$ m thick slice of freshly chopped frog liver sitting on top of the freezing head (Fig. 2). After the muscle was arranged neatly on the liver and its nerve was draped over two aluminum stimulating wires, it was finally blotted almost dry. Then, quickly, the whole muscle mount was plugged into the freezing machine and dropped onto an ultrapure copper block (Asarco Grade A-58), which had been precooled to 4°K by a spray of liquid helium from a

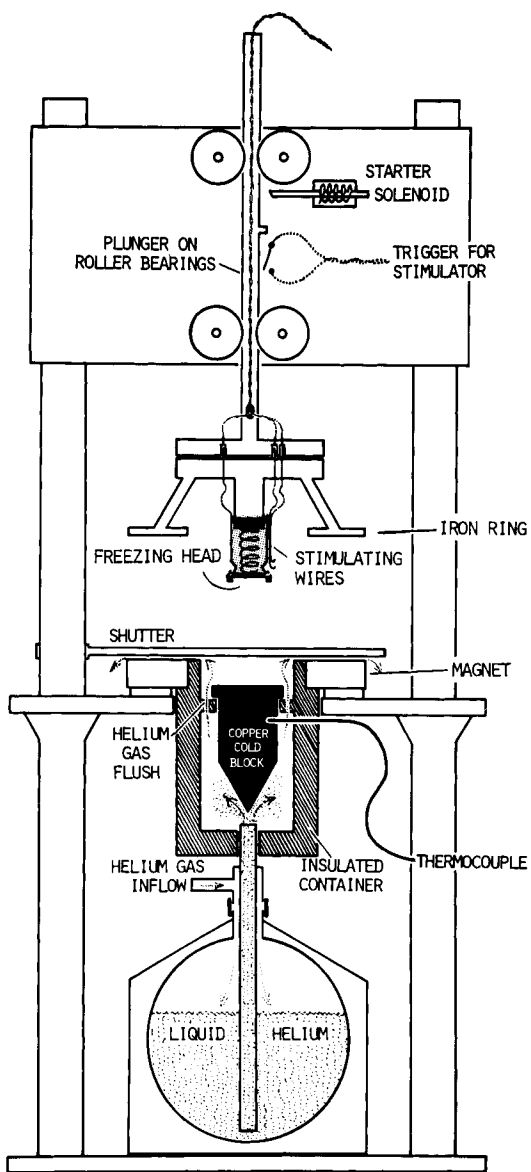


**FIGURE 1** Diagram of the freezing machine which smashes tissue against a super-cold metal block. The tissue is mounted on a freezing "head" which plugs into the end of a long plunger. The plunger is suspended above a block of ultrapure copper which is cooled to 4°K by spraying it with liquid helium. Once the tissue is mounted, the rod is released into free fall and glides down on ball bearings until the tissue strikes the cold copper block. The tissue is stimulated during the fall by wires incorporated in the freezing head, which connect to a stimulator that is activated by a magnet mounted on the plunger itself. The head is detachable so that the muscle can be mounted initially under a dissecting

storage Dewar mounted beneath the machine. The block temperature was monitored by a thermocouple plugged into it (Fig. 1). To prevent the muscle from drying or becoming chilled while it was mounted on the freezing machine, the mount was covered by a small moist styrofoam bucket (not shown) until just before freezing.

A critical requirement was that the timing between the moment of nerve stimulation and the moment of freezing could be set with a high degree of accuracy. To accomplish this, the tissue plunger was released by tripping a solenoid and fell smoothly on roller bearings (Fig. 1). As a result, the rate of tissue descent toward the copper block was remarkably similar from run to run. A magnet mounted on the plunger tripped an adjacent reed relay as the plunger was falling. This, in turn, activated a Grass stimulator (Grass Instrument Co., Quincy, Mass.) which delivered a supramaximal stimulus to the nerve. Reproducibility in the interval between stimulator activation and tissue impact against the copper freezing block was  $\pm 0.2$  ms. The location of the reed relay along the path of descent could be changed to vary the interval between stimulation and impact. In this way, intervals from 0 to 0.5 s could be set mechanically and additional fine adjustments could be made with the delay setting on the stimulator. The particular interval for each experiment was measured by starting the oscilloscope sweep at the same moment that the stimulator was activated. This allowed the stimulus and the moment of impact, signaled by closure of the oscillator or resistance circuits described in Appendix 1, to be recorded on the same oscilloscope sweep. Appendix 1 describes how these latter circuits were used to determine the rate of tissue freezing after impact.

#### Freeze-Fracturing

After the tissue was dropped against the freezing block, the plunger was separated from the freezing head so that the head could be quickly transferred into liquid nitrogen. Under liquid nitrogen, the aluminum disc was separated from the freezing head and the plastic ring was pulled off of the disc. The muscle remained firmly frozen to the filter paper which was epoxied onto the disc (Fig. 2). Discs were stored in liquid nitrogen until time for

microscope, and can be removed easily after freezing (see Fig. 2). The cold block is kept free from condensation of atmospheric gasses or water vapor by blowing helium gas over its surface (utilizing the vapor generated by the spray of liquid helium). Helium is confined to the region of the block by a shutter which opens at the last possible moment during the plunger's fall. The spray of liquid helium against the copper block is produced by pressurizing the liquid helium Dewar underneath the freezing machine. The temperature of the copper block is monitored with a copper-constantan thermocouple. The copper block is removable from above, because it must be warmed and dried between runs.

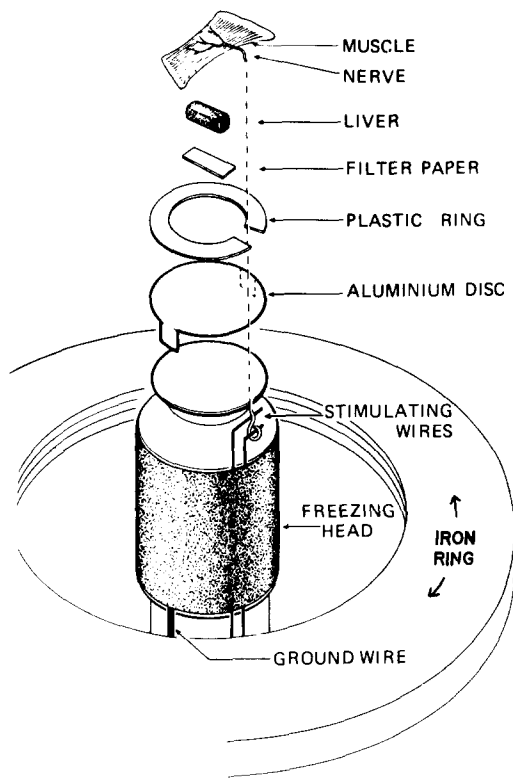


FIGURE 2 Exploded view of a muscle mounted on the freezing head ready to be stimulated and frozen. The muscle lies on a piece of liver to cushion its impact with the copper block and to raise its surface above the plastic ring. The liver sits on a slip of filter paper glued to an aluminum disc shaped to fit on the cold stage of a Balzers freeze-fracture apparatus. The filter paper absorbs some of the Ringer solution that clings to the liver and muscle, and when this Ringer's becomes frozen it bonds the liver and muscle tightly to the aluminum disc. The plastic ring prevents the muscle from being flattened beyond the reach of the knife in the Balzers microtome. (Whether the plastic ring is used or not, only the liver becomes squashed because the muscle fibers freeze so rapidly.) The nerve to the muscle is stimulated by aluminum wires attached through an isolation unit to a Grass stimulator. The ground wire soldered to the aluminum freezing head is part of a signal circuit used to monitor the exact moment at which the muscle contacts the copper block (Fig. 18). At the time of impact, the freezing head telescopes against the spring mounted inside it until the iron ring hits the electromagnet surrounding the copper block. The magnet prevents the freezing head from bouncing away from the copper block after impact. The iron ring is covered by a thin layer of foam rubber to cushion its impact with the magnet.

fracture, when each was transferred onto the four-position specimen stage of a Balzers 301 freeze-fracture apparatus (Balzers Corp., Nashua, N. H.), which the disc was designed to fit. To accomplish this transfer without warming the tissue surface, the muscle was first coated with frozen Freon 22, which melted during transfer and kept the surface of the muscle submerged in  $-150^{\circ}\text{C}$  Freon.

Inside the Balzers apparatus, the muscles were maintained at  $-105^{\circ}\text{C}$  for  $1/2\text{--}2$  h during pumpdown. Once a vacuum of  $2 \times 10^{-6}$  Torr or better was reached, each frozen muscle was fractured very superficially, with great care, by just barely grazing it with a specially sharpened razor blade which was new for each run. The fractured muscle was allowed to etch for 30 s, still at  $-105^{\circ}\text{C}$ , before it was replicated with platinum-carbon from the standard electron beam gun. The replicated muscle on its aluminum disc was then removed from the Balzers and plunged into methanol slush at  $-97^{\circ}\text{C}$  and allowed to warm slowly to room temperature. This effected a freeze dehydration, which in a sense fixed the muscle (8) so that it did not contract when it thawed with half of its membranes torn away. If such contraction were not prevented, it destroyed the delicate replica.

#### *Electron Microscopy*

Once thawed, the freeze-fractured muscle and its underlying filter paper were scraped off the aluminum disc and plunged into Purex-brand hypochlorite bleach which promptly released the replica from the underlying muscle. Usually, the replica was much too large to fit on a standard 3-mm specimen grid, so it was broken into pieces in the bleach, transferred to clean water, and picked up piecemeal. Typically, we could find only two to three nerve terminals upon a patient search through all of the fragments from any one muscle. So to get a large enough sample to ensure confidence in a result, three to four muscles were treated identically each day, on 2 or 3 d.

Replicas were examined at 80 kV with 50–100  $\mu\text{m}$  objective apertures in a JEM 100B or 100C. Photographs were taken of the entire extent of every nerve terminal that was not too badly damaged by ice crystals.

Features were counted, distances measured, and areas calculated directly from electron micrographs mounted on a Hewlett-Packard digitizing table (Hewlett-Packard Co., Palo Alto, Calif.); the table fed into a Hewlett-Packard 9810 table calculator programmed for statistical tests. These tests are discussed in Results; unless otherwise referenced, they were used as described in standard texts (48, 49).

#### *Electrophysiology*

Muscles were pinned to a thin layer of Sylgard covering the bottom of a shallow chamber. Their nerves were sucked into a stimulating electrode so that the length of nerve between the electrode and the muscle was the

same (1 cm) as that between the stimulating electrodes and muscles in the quick-freezing apparatus. The muscles were viewed with Zeiss-Nomarski optics, with a  $\times 40$  water immersion lens, which allowed ready visualization of unmyelinated nerve terminals at neuromuscular junctions. All experiments were performed at room temperature.

Intracellular recordings were made with potassium acetate-filled micropipettes of 10–30 M $\Omega$  resistance. The signal was fed into a W-P Instruments preamplifier (W-P Instruments, Inc., New Haven, Conn.) and displayed in a conventional manner. Extracellular recordings of focal end plate current were made with sodium chloride-filled micropipettes broken to tip diameters of 3–6  $\mu\text{m}$ . These were placed under visual control directly against an unmyelinated nerve terminal. To avoid recording “non-specific endplate currents” (cf. references 33 and 34), a second micropipette of the same size was placed against the surface of the same muscle fiber, within 50  $\mu\text{m}$  of the first pipette but away from any nerve terminal. The signal recorded by this pipette was amplified as described above, and the difference between the two signals was displayed on the oscilloscope screen.

## RESULTS

### I. Physiological Effects of 4-AP

Some of us knew from previous work that transmitter release at neuromuscular junctions in *Drosophila* larvae was substantially enhanced by 4-AP (29), and so we got together to try it on the frog. Muscles equilibrated in a sufficient concentration of d-tubocurarine ( $2 \times 10^{-6}$  M) to block all nerve-evoked contraction gave vigorous twitches when 1 mM 4-AP was added to their bath. It was necessary to increase the concentration of curare by 50 times to block nerve-evoked twitch in this concentration of 4-AP.

The profound enhancement of transmitter release which underlay the above observations was revealed by intracellular recording. Fig. 3 shows two endplate potentials (EPPs) recorded from the same curarized neuromuscular junction in the absence and presence of 1 mM 4-AP. Several features of this typical response to 4-AP are striking. First is the enhancement of the EPP amplitude, here ~20-fold. Second is its prolongation. Third is the appearance of a second and third peak on the falling phase of the EPP, roughly 5 and 10 ms after the initial peak (Fig. 4). This latter characteristic indicated that 4-AP not only enhanced the amount of transmitter released by a single stimulus, but also induced several bursts of release, perhaps by producing multiple action potentials in the nerve terminal. To test this latter

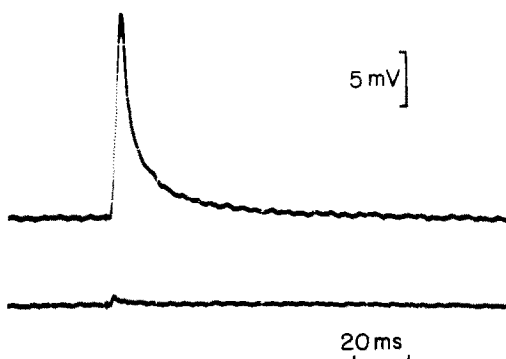


FIGURE 3 Intracellular EPPs recorded from a single muscle fiber in  $10^{-4}$  M curare and 10 mM  $\text{Ca}^{++}$ , before (below) and after (above) exposure to 1 mM 4-AP. The increase of transmitter output produced by 4-AP is about 50-fold.

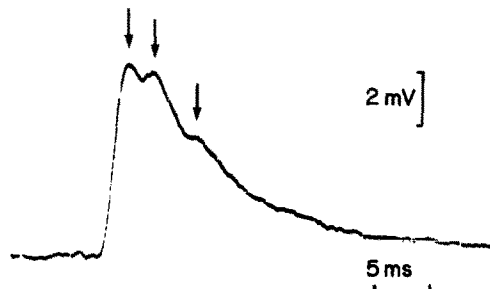


FIGURE 4 Intracellular EPP recorded from a curarized muscle fiber exposed to 1 mM 4-AP in Ringer's containing the normal, low level of 2 mM calcium. The duration of such “giant” 4-AP EPPs in 2 mM calcium is far longer than normal, and many, such as this one, have three distinct peaks (arrows), suggesting that the axon fired repetitively.

possibility, we used focal extracellular recording, and confirmed that a single nerve stimulus did produce multiple action potentials in the nerve terminal (Fig. 5). Usually, there were two or three nerve terminal spikes at  $\sim 5$ -ms intervals (indicated by arrows in Fig. 5); successive spikes released progressively less transmitter, as revealed by the amplitudes of the postsynaptic response. We do not know why 4-AP causes this repetitive firing.

Since one of the purposes of the present investigation was to look for exocytosis as a function of time after impulse arrival, it was clearly detrimental to have this repetitive response of the axon terminals. To circumvent this difficulty, we made use of the fact that elevated concentrations of divalent cations increase the threshold for initia-

tion of an action potential in axons (22). Raising the concentration of calcium in the bathing medium to 10 mM prevented the repetitive firing. In that condition, extracellular recordings of evoked responses showed a single peak of current (Fig. 6). Thus, all of the morphological studies were done on muscles stimulated in 10 mM calcium.

The main point of interest in Fig. 6 is the time-course of the endplate current. It reaches its maximum 4–5 ms after nerve stimulation and continues for another 2 or 3 ms. Since this is an extracellular record, it should be an accurate

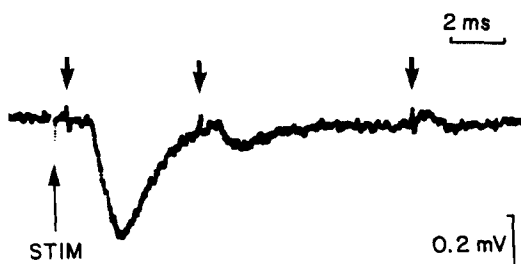


FIGURE 5 Extracellular recording from a curarized neuromuscular junction exposed to 1 mM 4-AP in normal, 2 mM calcium Ringer's confirms that, at this level of calcium, the axon fires repetitively after a single stimulus. This record reveals three tiny biphasic spikes (arrows) just before the larger downward deflections which represent the postsynaptic endplate currents; these tiny spikes represent three successive action potentials in the nerve. Such repetitive firing was prevented in subsequent experiments by raising calcium outside the nerve to 10 mM.

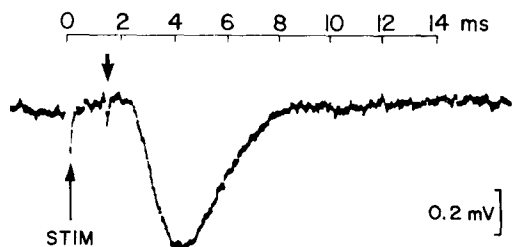


FIGURE 6 Extracellular recording from a curarized neuromuscular junction bathed in 1 mM 4-AP and 10 mM  $\text{Ca}^{++}$  and given a single electrical stimulus at the lower arrow. The tiny biphasic spike ~1.5 ms after the stimulus (upper arrow) represents the nerve action potential. The large downward deflection which began 1 ms later represents the postsynaptic endplate current evoked by acetylcholine discharged from the nerve. This trace reveals that acetylcholine release from 4-AP-treated nerves is not only much greater than normal, but also lasts longer. Normal postsynaptic endplate currents are over by 5 ms. Presumably, this occurs because 4-AP prolongs the action potential and holds open the calcium channels in the presynaptic membrane longer than usual.

monitor of the time-course of evoked transmitter action.<sup>1</sup>

## II. Structural Effects of 4-AP

On the basis of recordings of endplate current such as illustrated in Fig. 6, we chose the interval 3–6 ms after nerve stimulation as a likely time to look for synaptic vesicle exocytosis. This would allow 1–2 ms for action potential conduction from the stimulating electrodes to the terminals, and 1 ms for the synaptic delay that precedes transmitter release (32), so it ought to catch the endplate current near its maximum. (Of course, in attempting to freeze the tissue at a chosen interval after nerve stimulation, we had to worry about the delay between the time when the muscle hit the freezing block and the time when it actually froze. When we began this study, we did not know how to measure this freezing delay, but inferred that it was <10 ms (28). In Appendix 1, we describe a new method for measuring freezing rates which gives values that agree with this assumption.)

From our first experiment on, every muscle that was bathed for 30 min in 1 mM 4-AP and given one stimulus ~5 ms before impact against the freezing block yielded abundant images of what looked like holes or pores in the presynaptic membrane (Fig. 8). These images were not visible in muscles that were stimulated 3 ms or less before impact (Fig. 7). Moreover, they were never found in control muscles bathed in 2 mM 4-AP for similar times and quick-frozen without any stimulation. As would be expected, thin-section views through active zones of synapses from muscles treated in a similar manner showed pockets in the presynaptic membrane which looked like synaptic vesicles in exocytosis (25). Thus, we will hereafter describe the freeze-fracture images in question as "vesicle openings," to indicate that we think they are exocytotic stomata.

In every muscle stimulated at such early times, however, we observed some nerve terminals that displayed no vesicle openings at all. In fact, in

<sup>1</sup> One of the reviewers of our original manuscript, who helped tremendously with the style and content of this paper but preferred to remain anonymous, added at this point: "It is universally inferred that transmitter action is closely related to the time-course of release (cf. reference 32), but the relationship between release and action is not known from direct observation. This is one of the points of interest in this paper; a second plausible measure of the time-course of release can at least be contemplated."

several muscles as many as a quarter of all the terminals displayed no openings. But this was true only when stimulation was delivered in the last 10 ms before impact; when stimulation was given earlier, >95% of the nerves showed signs of vesicle openings.

We presume that the problem with intervals <10 ms was that the muscles were so close to the freezing block at the time of stimulation that their incoming nerve trunks, which stood a bit above the surface, became unduly chilled by the cloud of cold helium gas that surrounded the block, and

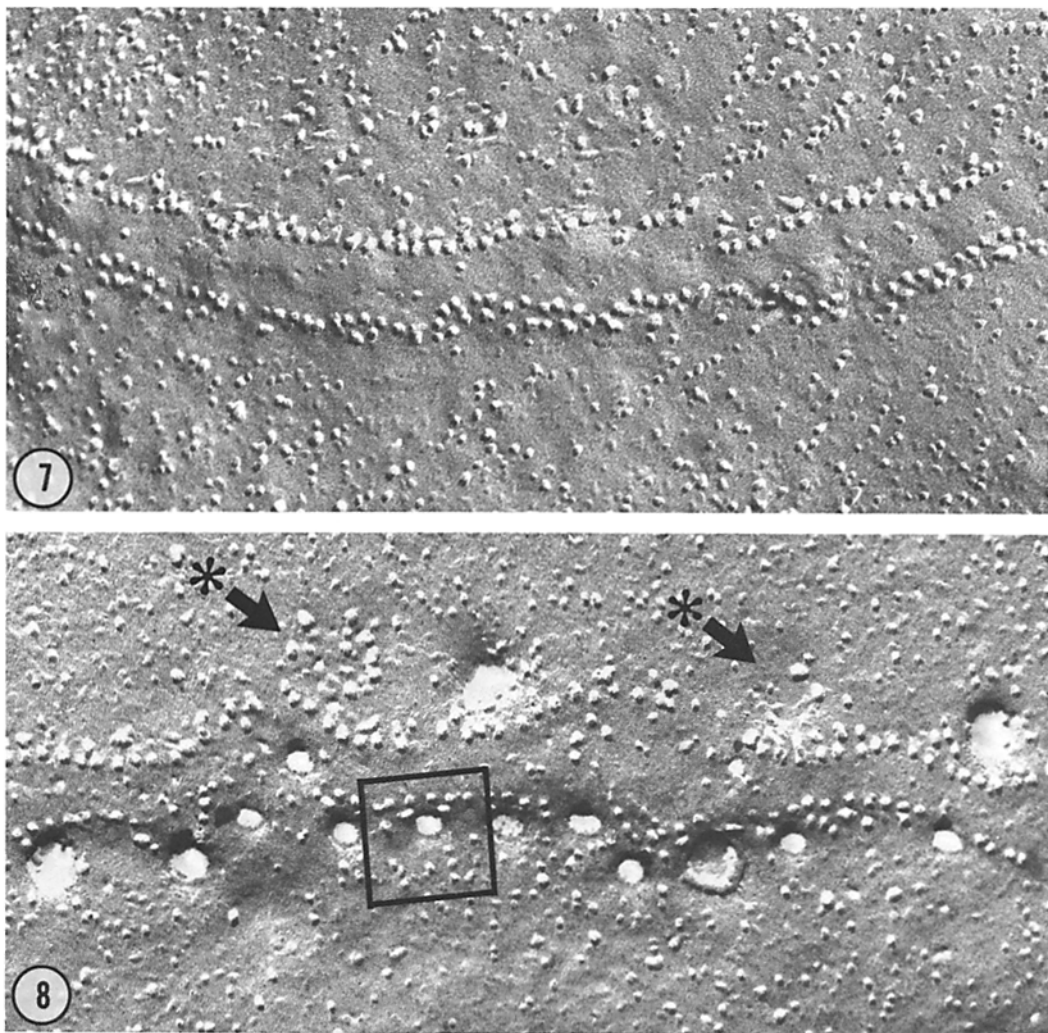


**FIGURE 7** High magnification view of the "P face" of one active zone from a frog motor nerve terminal soaked in 1 mM 4-AP and 10 mM  $\text{Ca}^{++}$  for 30 min and given one stimulus 3 ms before freezing. By 3 ms, the action potential presumably arrived in the terminal, but it did not alter the resting appearance of the active zone, which is recognized as a slight ridge bordered by parallel rows of large intramembrane particles.  $\times 143,000$ .

**FIGURE 8** P-face view of an active zone from a nerve terminal treated like the one in Fig. 7, but given one nerve stimulus 5 ms before freezing. In the interval between 3 and 5 ms, just at the time when the nerve begins to discharge large numbers of acetylcholine quanta, many membrane perturbations appear along the edges of the active zone. We believe that these are exocytotic stomata, or openings into the underlying synaptic vesicles. The two areas marked by asterisks we think are vesicles that have collapsed flat after opening; they display a telltale cluster of two or more large intramembrane particles like those found in intact synaptic vesicle membranes. The area in the square illustrates the characteristic domain of exocytosis portrayed graphically in Fig. 16.  $\times 143,000$ .

failed to conduct the nerve impulse. (It must be realized that the muscles accelerated during their descent to  $>1$  mm/ms, so an interval of 5 ms meant that they were stimulated when  $<5$  mm away from the block.) The original design of our freezing machine did not allow us to stop the flow of cold helium gas completely enough to avoid such prechilling of the muscles. Though we later took pains to avoid it, we presume that it happened to a greater or lesser extent to all the muscles we studied. In Fig. 18 of Appendix 1, we document a  $10^\circ$  temperature drop in the last ms before impact, by placing a hairlike 25- $\mu\text{m}$  thermocouple on the surface of a test muscle. Later, in Section IV, we will duly consider how this cooling before impact might contribute to the slight disparity between the physiological and morphological results that will emerge.

### *III. Vesicle Openings Compared with Quanta*

For quantitative analysis, 10 muscles were soaked in 1 mM 4-AP and stimulated at intervals of 4.5–5.5 ms before impact against the copper freezing block. Nerves were located in freeze-fracture replicas, and the number of synaptic vesicle openings was counted at all the well-frozen active zones that showed any signs of activity at all. Also, the length of each active zone was measured, to give the number of vesicle openings per  $\mu\text{m}$  of active zone. In the four best frozen muscles, where 208 active zones were found, the mean number of vesicle openings per  $\mu\text{m}$  of active zone was 11.5, 11.7, 12.9, and 16.4; so the overall mean, weighted for the numbers of active zones in each group, was  $12.9 \pm 2.3$  vesicle openings/ $\mu\text{m}$  of active zone.

To extrapolate these numbers to whole neuromuscular junctions, it was necessary to know how many  $\mu\text{m}$  of active zone are present in all the nerve terminal branches that comprise an average endplate. To determine this, we reacted 10 tiny muscles (the size we used in quick-freezing) for cholinesterase histochemistry (37) and measured the extent of the staining, which closely matches the distribution of nerve terminals. Light microscopy of whole mounts of these 10 muscles yielded good images of 90 endplates. Each was composed of two or more terminal nerve branches. Adding together the length of all the branches at each endplate gave a mean total length of  $300 \pm 109$  (SD)  $\mu\text{m}$  per endplate. Then we turned to the freeze-fracture views of nerve terminals, and

measured how often active zones occurred along their length and how wide each active zone was. There was considerable variability in these morphological features; active zones ranged in length from  $<0.1$   $\mu\text{m}$  to  $>3.0$   $\mu\text{m}$ ; but, on the average, they were  $\sim 1$   $\mu\text{m}$  long and were spaced slightly  $<1$   $\mu\text{m}$  apart. This gave a mean of 1.4  $\mu\text{m}$  of active zone per running  $\mu\text{m}$  of nerve terminal. Hence, the average nerve terminal in these tiny muscles had  $300 \pm 109$  times 1.4, or  $420 \pm 130$  (SD)  $\mu\text{m}$  of active zone. This meant that, on the average,  $\sim 12.9$  vesicles/ $\mu\text{m}$  of active zone times 420  $\mu\text{m}$  of active zone/nerve terminal, or  $\sim 5,500$  vesicles/nerve terminal, underwent exocytosis as a consequence of one nerve stimulus in 1 mM 4-AP.

We would have liked to measure the quantal content of the EPPs in 1 mM 4-AP, but we could not do so accurately because they were too large for the variance method, and they fatigued too fast upon repetitive stimulation (Fig. 9). Important presynaptic changes may be heralded by this fatigue. First, depletion of the pool of transmitter immediately available for release probably occurs (15), since the first discharge is so massive. Second, 4-AP may dissociate from the axon during each action potential. Studies of the effects of 4-AP on squid axon have shown that prolonged depolarization does dissociate 4-AP from the membrane (59). However, much of this fatigue may be due to postsynaptic changes. There is now considerable reason to suspect that curare or 4-

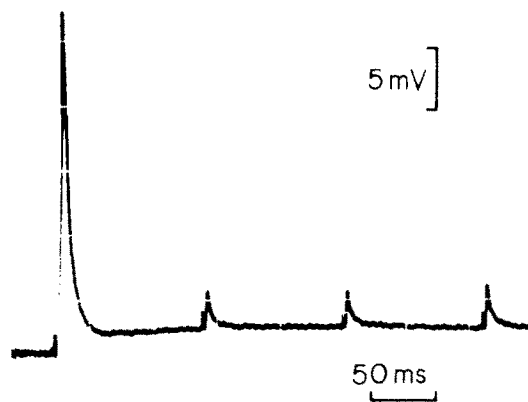


FIGURE 9 Intracellular record of the first four EPPs evoked by stimulating a neuromuscular junction at 10 Hz after soaking it in 2 mM 4-AP. Only the first EPP is a giant one; subsequent ones are greatly depressed and ride on an elevated baseline membrane potential, for which we have no explanation.

AP, or both, may plug the postsynaptic receptor channels when they open in response to the first pulse of acetylcholine and keep them plugged long enough to render them unresponsive to subsequent acetylcholine pulses (39, 42, B. Katz, personal communication).

In the absence of a good voltage clamp, we were forced to estimate quantal contents in 4-AP by one of two approaches. First was to measure relative EPP amplitudes in curare. A muscle in 10 mM calcium was curarized to a level which just barely blocked contraction to indirect stimulation. Then, a fiber in this muscle was impaled with an intracellular micropipette, and EPPs were recorded in response to 100–200 stimuli. From the variance in the amplitudes of these EPPs, their mean quantal content was estimated. The recording electrode was then withdrawn and the concentration of curare was increased 50-fold, enough to prevent twitching even in the presence of 4-AP. After equilibration, the same fiber was penetrated again and the reduced amplitude of its EPP in the elevated curare concentration was noted. The electrode was again withdrawn, and 1 mM 4-AP was added to the bath and allowed to equilibrate for at least 20 min. Finally, the same fiber was impaled a third time and the amplitude of its first response to nerve stimulation in 4-AP was recorded. To estimate the quantal content of the EPP in 4-AP, we divided its amplitude by the amplitude of the previous EPP recorded at the same curare level without 4-AP, and multiplied this quotient by the quantal content originally estimated at the lower curare concentration. By this method, we found approximately a 30-fold increase in response amplitude in 1 mM 4-AP, at endplates which had quantal contents of 100–200 before its addition. Thus, we concluded that in 10 mM calcium and 1 mM 4-AP, a single nerve impulse released ~30 times 100–200, or 3,000–6,000 quanta.

In the face of several uncertainties with this method of estimating the number of quanta, which are described in the next section, we used another measure of the increase in acetylcholine release produced by 4-AP. The concentration of curare needed just to block the muscle twitch in 1 mM 4-AP was compared to the concentration needed to block twitch in normal Ringer's. This dose-ratio was then used to calculate the amount of acetylcholine released in the presence of 4-AP, relative to release in its absence. These calculations were based on simple first-order kinetics and are given

in Appendix 2. They provided an independent measure of the augmentation of acetylcholine release in 4-AP, which we could again multiply by the normal quantal content (100–200 quanta per impulse) to obtain an estimate of the quantal content in 4-AP. For example, the curare dose-ratio for the change from 0 to 1 mM 4-AP indicated that acetylcholine release increased 40-fold, which would argue that 40 times 100–200, or 4,000–8,000 quanta were released per impulse. Thus, two independent estimates of the number of quanta released at a neuromuscular junction in 1 mM 4-AP gave values (3,000–8,000) similar to the morphological counts of the number of synaptic vesicles that were caught in an open configuration by quick-freezing.

#### IV. Potential Sources of Error

Several factors disturbed these efforts to correlate the physiological estimates of quantal output with the morphological counts of vesicle openings. Most important, several facets of the physiological experiments probably led us to underestimate the augmentation in quantal output produced by 4-AP; that is, quantal output may have increased much more than we thought. First, we compared only the peak amplitudes of EPPs before and after 4-AP, not the total endplate currents; so our estimates of augmentation did not take proper account of the prolonged duration of quantal release that occurs in 4-AP. (Nevertheless, it was quite apparent that quanta are discharged at high levels for much longer than normal after a nerve impulse in 4-AP, because the rising phase of the endplate current was very prolonged [Fig. 6].) Initially, we disregarded this prolongation and presumed that it would be more appropriate to correlate the peak rate of quantal release with the peak concentration of vesicle openings captured at the height of the endplate current. That was because we imagined that synaptic vesicle exocytosis would be such a rapid event that quick-freezing would only sample the momentary rate of secretion. But, since then, we have learned that each exocytotic event lasts a relatively long time in 4-AP, compared to the total duration of the endplate current (25). Thus, vesicle openings must accumulate during each secretory burst in 4-AP. Indeed, we could have compared the maximum concentrations of openings at the end of the EPP with the total number of quanta released, taking account of both the increased amplitude

and the increased duration of discharge in 4-AP, instead of catching the peaks, as we did.

Regardless, we may still have underestimated the peak rate of quantal release, because the 4-AP-augmented EPPs often reached 20 mV or more, so nonlinear summation of the individual quantal amplitudes must have occurred (41); but we did not correct for this. Moreover, we noted that 4-AP itself exerted a visible curarizing effect on miniature endplate potentials (MEPPs) at 1 mM concentration, which must have depressed postsynaptic response and obscured some of the increase in presynaptic release; but we did not know how to correct for this. Another problem was that all our measurements were based on the assumption that acetylcholine and curare compete for the receptor by classical first-order kinetics; but subsequent to our work it was discovered that curare not only competes with acetylcholine for binding to the postsynaptic receptors, but also plugs or occludes the receptor-mediated ion channels after acetylcholine opens them (39, 42, B. Katz and R. Miledi, personal communication). Especially at high doses of acetylcholine and curare, such channel-plugging may become a significant part of curare's blocking action. If this occurred in our studies, then both the EPP augmentation and the dose-ratio approaches would give very severe underestimates of how much quantal discharge was augmented by 4-AP. However, to date, this channel-blocking effect of curare has been seen only when the postsynaptic membrane is hyperpolarized and acetylcholine is applied ionophoretically. It has not shown up in the classical studies of the effects of nerve-released acetylcholine on the muscle (30). So we still do not know whether we should have corrected for it. Taken together, these various potential problems raise suspicion that we did underestimate how much 4-AP increases acetylcholine release. Recently, B. Katz and R. Miledi (personal communication) have observed quantal contents in excess of 100,000 by voltage clamping frog neuromuscular junction after exposure to 3,4-diaminopyridine.

But before concluding that there may have been more quanta released than vesicles opened, we should take into account that muscles mounted on the freezing machine probably did not release as many quanta as the muscles exposed to 4-AP in our physiological experiments. Muscles were mounted slack on the freezing head, and such release of a muscle's normal resting tension is known to decrease acetylcholine release (in our

hands, by roughly 25%). Moreover, during the plunge, the muscles were on the verge of drying out; and at the last moment, just as they were stimulated, they got blasted with the exhaust of cold helium gas (so much so, that some nerve terminals failed to release anything, as was pointed out above). Certainly, these deleterious conditions could have depressed quantal release to as great an extent as we underestimated its increase in 4-AP; in which case, the two errors would cancel and the correlation of quantal and vesicle release would hold. Nevertheless, in the face of these uncertainties, we sought to demonstrate a consistent trend in the relationship between vesicles opened and quanta released at lower levels of discharge, where we expected that some of these errors would also be smaller.

#### *V. Vesicle Openings Compared with Quanta at Lower Doses of 4-AP*

The correlation between physiological estimates of quantal release and morphological counts of vesicle openings held fairly well as the dose of 4-AP was lowered (Table I). When 4-AP was reduced 10-fold, to 0.1 mM, the estimates of quantal content were diminished by a factor of 2.5, and the concentration of curare needed to block the twitch was 2.6 times smaller (Table III, Appendix 2). EPPs from four muscles in 0.1 mM 4-AP had quantal contents of between 1,800 and 3,800, while the estimate from the curare dose-ratio method was 1,850 quanta per impulse.

In four muscles, where 366 active zones were found, the mean number of vesicle openings per  $\mu\text{m}$  of active zone was 2.26, 3.83, 4.47, and 6.05; so the overall mean was  $4.4 \pm 1.6$  (SD). This multiplied by  $420 \pm 130 \mu\text{m}$  of active zone gave between 1,000 and 2,500 vesicle openings per nerve terminal, which was significantly less than the number of vesicle openings found after stimulation in 1 mM 4-AP (Mann-Whitney test). This difference was visibly apparent; compare Fig. 11 with Fig. 10. Thus, these estimates of the number of quanta released in 0.1 mM 4-AP (1,800–3,800) fit reasonably well with the number of synaptic vesicles we observed in the open configuration (1,000–2,500).

At 0.01 mM 4-AP, the EPP was 3–5 times greater than it was in normal Ringer's (Table I), and 3–4 times more curare than normal was needed to block muscle twitch (Table III, Appendix 2). Measurements of EPPs led to estimates of

TABLE I  
*Synaptic Vesicle Openings vs. Quantal Content*

(1) Concn of 4-AP (in 10 mM Ca <sup>++</sup> )	(2) Average quantal content of EPP	(3) Open and collapsed vesicles, per average endplate	(4) Just collapsed vesicles	(5) % Collapsed ves- icles	(6) No. of muscles	(7) No. of active zones
<i>M</i>						
0	180	130	126	99+	4	75
10 <sup>-5</sup>	700	800	320	40	4	77
10 <sup>-4</sup>	1,900	2,100	770	37	9	262
10 <sup>-3</sup>	4,600	5,300	1,200	23	2	26

Comparison between the number of quanta discharged (estimated by the curare dose-ratio method in Appendix 2) vs. the number of vesicles caught in the act of exocytosis (both those that are wide open and those that have collapsed) in three concentrations of 4-AP. Column 2 should be compared with column 3 to see how good the correlation is. Column 5 illustrates that it becomes progressively harder to catch vesicles in the wide-open state as 4-AP concentration is reduced and the total number of vesicle openings declines.

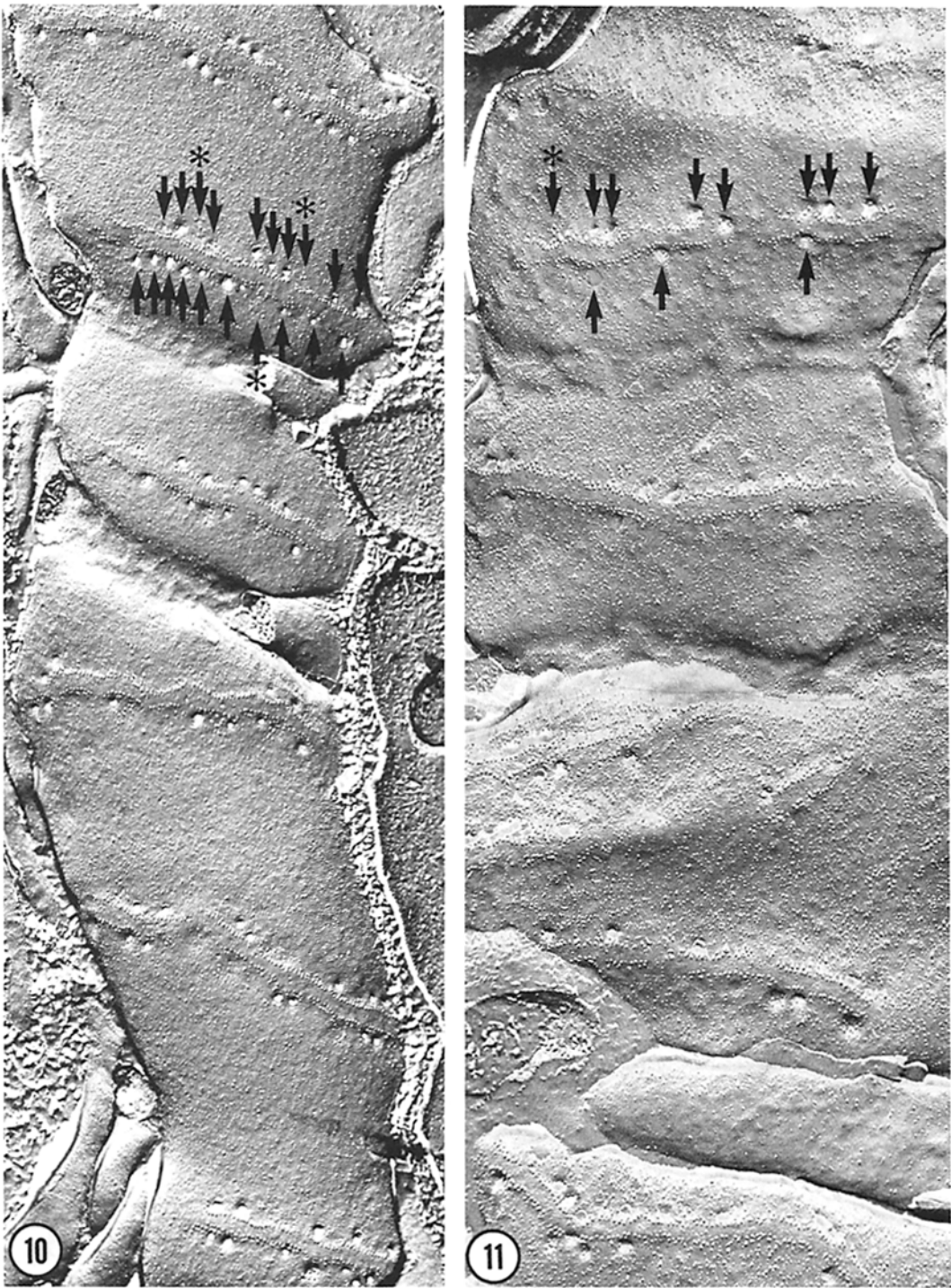
quantal content of 600–1,500, while the estimate from the curare dilution method was 680 quanta per impulse. In muscles stimulated in this low dose of 4-AP, the number of nerve terminals that showed no structural change was higher than in 1 mM 4-AP (70% instead of 25%). However, 328 active zones from nerve terminals in four muscles which did show some activity had 0.20, 0.39, 0.59, and 1.61 vesicle openings per  $\mu\text{m}$  of active zone, which gave a mean for these “responsive” terminals of 0.56 vesicle openings per  $\mu\text{m}$  of active zone. Multiplied by 420  $\mu\text{m}$  of active zone in all, this gave between 150 and 300 vesicle openings per nerve terminal, which was significantly less than the number of openings found after stimulation in 0.1 mM 4-AP, as could easily be seen by comparing replicas such as Fig. 12 and Fig. 11. However, this number of vesicle openings was too low to correlate well with our best estimate of the number of quanta released in 0.01 mM 4-AP (600–1,500).

#### VI. Difficulties in Finding Vesicle Openings in the Absence of 4-AP

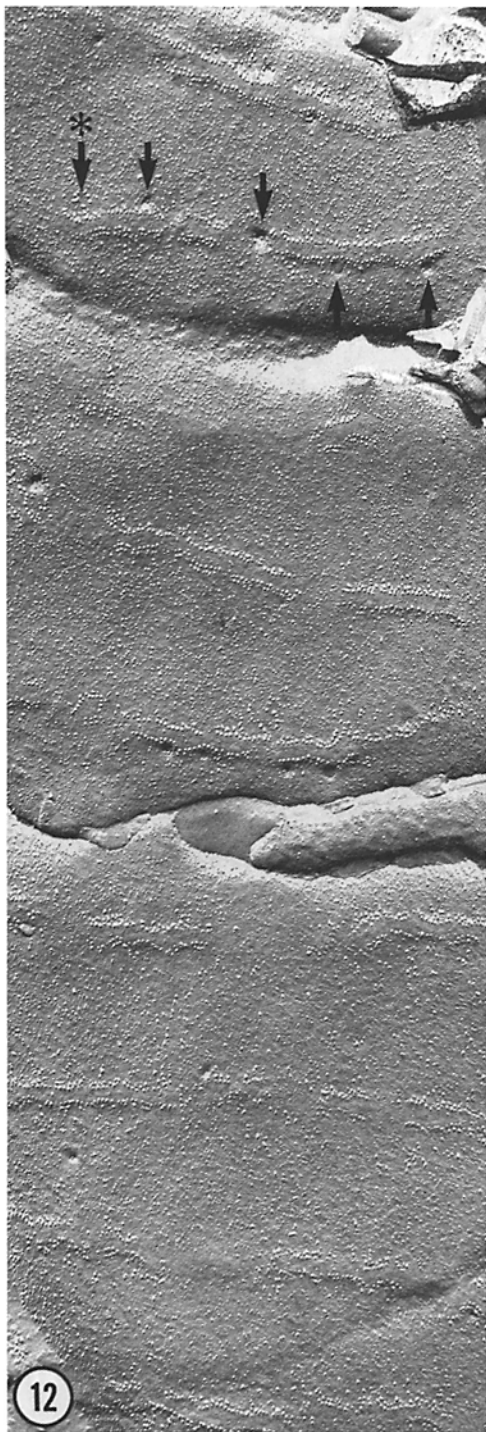
Vesicle openings were extremely rare after a single stimulus in Ringer's containing 10 mM calcium without any 4-AP. We searched for them in vain through a whole range of stimulus-freezing intervals, between 3 and 7 ms, in 56 different muscles (Fig. 13). In fact, only two of these muscles, frozen at 4.0 and 4.5 ms after a single stimulus, had any of the plasmalemmal pockets we had become used to seeing in 4-AP; and the terminals in these two muscles still displayed only

four vesicle openings per 100 active zones. In contrast, the physiological determinations of numbers of quanta released in the absence of 4-AP (~200 in 10 mM calcium) led us to expect one vesicle opening for every two to three active zones. So, as reported previously (28), under normal conditions there was a considerable discrepancy between the number of vesicles caught in exocytosis and the number of quanta released: far too few vesicle openings. This same discrepancy also emerged in high doses of 4-AP, when quantal release was held down to normal levels by replacing 10 mM calcium with 9.5 mM magnesium and 0.5 mM calcium. Under these conditions, vesicle openings were extremely rare; again, <0.1 per  $\mu\text{m}$  of active zone. (It is important to stress that these high Mg<sup>++</sup>/low Ca<sup>++</sup> experiments also served as controls against the unpleasant possibility that the observed vesicular exocytosis at higher rates of output was simply an artifact of 4-AP.)

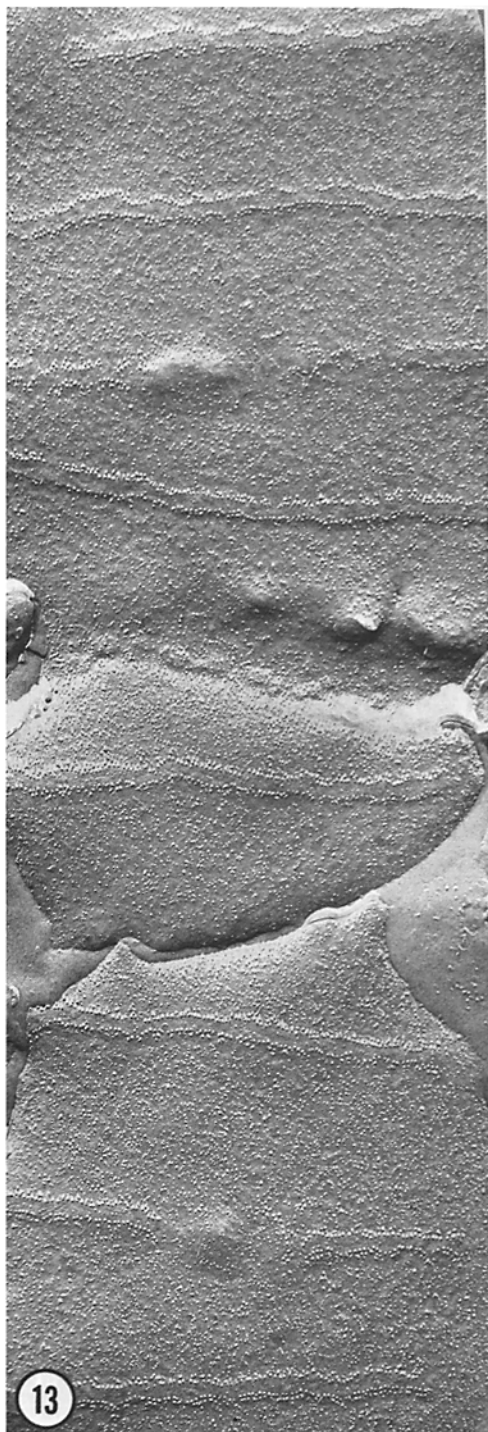
The reason for the discrepancy between numbers of vesicle openings and numbers of quanta at normal levels of release became clear only after we had completed the above counts and we began to study the fate of discharged vesicles, which we did by progressively increasing the interval between stimulation and freezing. It became apparent that vesicles collapse or flatten out after they open; and, as a result, they deposit in the plasma membrane a cluster of two to four large intramembrane particles which were originally a part of their own membrane. So, for example, in terminals frozen 20 ms after stimulation in 4-AP, their



FIGURES 10-13 Low magnification views of the P faces of frog nerves given one single shock 5-6 ms before quick freezing, in different doses of 4-AP. In each figure, the arrows point to all the examples along one active zone that we counted as either vesicle openings (plain arrows) or collapsed vesicles (arrows with asterisks), in gathering the data for Figs. 14 and 15. Fig. 10 illustrates the great abundance of exocytosis that occurs in 1 mM 4-AP. Each active zone is flanked by many vesicle openings, but no openings are found anywhere else on the nerve terminal surface. Fig. 11 illustrates that exocytosis is considerably less abundant in 0.1 mM 4-AP, but a number of openings still occur at each active zone. This is a good level of output to test for nonrandomness in the location of vesicle openings along each active



12



13

zone, or to test for variations in activity from active zone to active zone (see text). Fig. 12 illustrates the low incidence of exocytosis after stimulation in 0.01 mM 4-AP. Some active zones display no exocytic figures, while others display a few. This distribution appears to be totally random; there is no indication that active zones discharge in an all-or-none fashion (see text). Fig. 13 illustrates the apparent lack of exocytosis in terminals stimulated in the absence of 4-AP. In spite of the fact that such terminals released 150 quanta in physiological tests, which would have been 1 quantum from every third active zone, obvious exocytotic vesicles rarely occurred with this frequency. All approx.  $\times 40,000$ .

telltale clusters of intramembrane particles have become quite numerous beside the active zones, while the more narrowly open synaptic vesicles have become less numerous (25), indicating that they are earlier stages of exocytosis. This collapse of the exocytic vesicle is the first step in vesicle membrane recycling and will be fully documented in a subsequent paper, but it is important to bring it up here because it turned out to affect quantitation in a manner which helped to resolve the apparent discrepancy between vesicle openings and quanta at low levels of release. When we went back to examine the aforementioned series of terminals frozen at 5–6 ms after stimulation, we realized that many telltale clusters of intramembrane particles were already present beside their active zones by 5 ms (see Fig. 6). This meant that some exocytotic vesicles must have already collapsed, but we had failed to count them as having opened. When we did include them in our counts of vesicle openings, it greatly improved the correlation with quantal release (Table I). This was particularly true at low levels of transmitter release, in normal Ringer's, where obvious vesicle openings were rare and the proportion of collapsed vesicles was very high. As transmitter release was augmented by progressive increases in 4-AP concentration, the absolute number of collapsed vesicles increased as well; but they became relatively less abundant than the more narrowly open vesicles. This relative increase in the images that we take to be the early stage of exocytosis would suggest that vesicles collapse more slowly in 4-AP than they do normally. We presume that the first vesicles which open in 4-AP collapse just as fast as in normal Ringer's but that, after a certain number of vesicles have done so, they alter the presynaptic membrane in such a way that subsequent vesicles (which continue to be discharged for many ms in 4-AP) collapse much more slowly than normal and thus become much easier for us to catch at an earlier stage of opening by quick-freezing. We consider such variations in vesicle collapse rate in more detail elsewhere (25), and will present in a subsequent paper the evidence that changes in the presynaptic membrane affect vesicle collapse. Here, it is important to stress that we believe vesicles collapse so fast in normal Ringer's that they are hard to catch in the wide-open configuration, even by quick-freezing; but when we count collapsed forms, then the correlation between vesicles and quanta presented in Fig. 14 is improved.

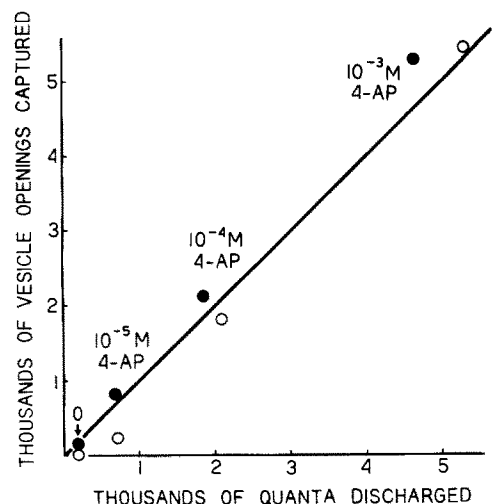


FIGURE 14 The number of vesicle openings captured by freezing 5–6 ms after a single shock, in three different concentrations of 4-AP, vs. the number of quanta discharged. The closed circles are the average number of vesicle openings found in our most extended views of terminals (in which collapsed vesicles could also be counted easily) vs. the number of quanta estimated by the curare dose-ratio method described in Appendix 2. The open circles are earlier data, the average of number of vesicle openings found in all the active nerves we saw (before we began to count collapsed vesicles), vs. the number of quanta estimated by recording EPPs. The diagonal line is the 1:1 relationship expected if each vesicle that opened released 1 quantum of transmitter. The points indicated by zero are the result of stimulating in normal Ringer's without any 4-AP.

## VII. Spatial Distribution of Vesicle Openings

The spatial distribution of vesicle openings was examined at the different levels of release in the various concentrations of 4-AP (Fig. 15). The most striking result was that exocytosis invariably occurred beside the double rows of particles that are aligned in the presynaptic membrane at the "ridges" which mark the location of the presynaptic dense bars seen in thin sections (Figs. 7, 8, and 10–13). The mean distance from the centers of vesicle openings to the innermost row of particles was  $420 \pm 74 \text{ \AA}$  (SD); the distribution of these distances is plotted in Fig. 16. Regardless of the concentration of 4-AP, we found no "ectopic" vesicle openings at the times used in this study. The total number of vesicle openings could always be accommodated in two rows on either side of each active zone (Fig. 15).

We then asked whether vesicle openings occurred along these rows in a random manner. We devised statistical tests for several nonrandom patterns of vesicle openings; those we considered are illustrated in Fig. 17. These tests treated the active zone as a linear series of domains, each wide enough to accommodate one vesicle, open or closed. Such partitioning fit well with Couetteaux's demonstration that vesicles line up in two regularly spaced rows on either side of the active zone, just inside the presynaptic membrane (13). The vesicles are  $\sim 500$  Å in diameter and do not quite touch each other, so they occupy a cytoplasmic domain somewhat  $>600$  Å. Correspondingly, we found that when vesicle openings were most abundant in the presynaptic membrane (as in Fig. 8), they were regularly spaced at an average distance of  $707 \pm 13$  Å (SD).

The results of the statistical tests are summarized in Table II. In the first three tests, we calculated the number of runs, pairs, or unilateral vesicle openings that would occur by chance, if the distribution were inherently random, at each level of activity (where activity was defined as the number of domains where exocytosis could have occurred relative to the number of openings actually seen). The observed deviations from the number expected by chance were then plotted (in  $Z$  units) on probability paper and tested against a normal distribution (Kolmogorov-Smirnov test). From Table II, it is apparent that these deviations were no greater than would be expected by chance variation in a random process.

At this point, we were concerned that interaction between vesicles might appear only at lower levels of release, when vesicle openings ought to be few and far between. This was examined by returning to the data from the 100 ridges used for the run test and reevaluating the data, taking account of the variability in activity (17–89% of the domains were occupied by vesicle openings). We found that the correlation coefficient ( $r$ ) between the level of activity and the deviations from the expected numbers of runs ( $Z$ ) was only 0.06, so there was no basis for supposing that runs occur only at lower levels of release.

The fourth and most sensitive test was to construct a serial correlogram (48) for each active zone (Table II). The statistic in this test was a series of five correlation coefficients ( $r$ ) for each zone. The first correlation coefficient was derived by imagining that each of the vesicle domains has been displaced laterally by one position in the

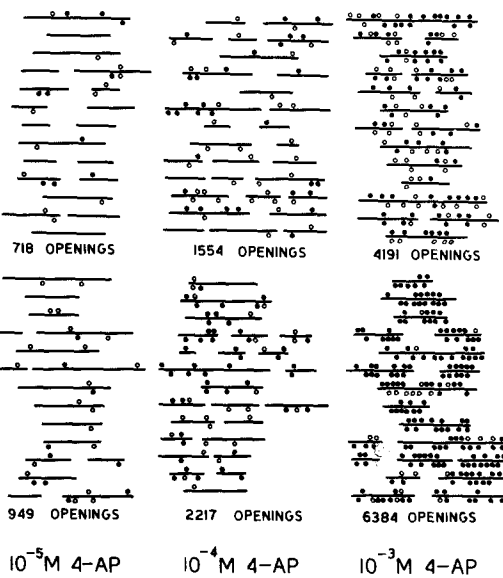


FIGURE 15 Typical maps of the distribution of vesicle openings (black circles) along the active zones (black lines) of six nerve terminals frozen  $\sim 5$  ms after a single shock in three concentrations of 4-AP. Numbers beneath each tracing are extrapolations of the observed density of vesicle openings in the regions illustrated, to whole neuromuscular junctions (which typically have  $\sim 300$  active zones), assuming that their activities were uniform. As shown in Fig. 14, these values correspond rather closely to the number of quanta released by a nerve terminal in each of these concentrations of 4-AP. The open circles represent vesicles that appeared to have collapsed after exocytosis.

active zone and asking whether the actual vesicle openings were correlated with the vesicle openings in the displaced condition. Clearly, if every fifth domain were especially likely to contain a vesicle opening, i.e., if openings were distributed nonrandomly, the correlation coefficient would jump to +1 (the highest possible correlation), when five displacements had been made. However, for up to five displacements, the correlation coefficient averaged  $<0.25$ , which was not significantly different from random, considering the limited number of active zones we analyzed. This inability to detect any patterning in the distribution of vesicle openings at individual active zones fit with the results of the other three tests, and all the tests argued that the distribution of vesicle openings at each active zone was random.

The next step in analyzing the spatial distribution of exocytosis was to measure the variation between active zones. We supposed that if each

active zone behaved as a unit, or even in an all-or-none manner, differences in activity between adjacent zones would have been greater than would be predicted by random variation. Because the level of activity varied significantly from one muscle to the next ( $t$  test;  $P < 0.01$ ), and also varied among the different nerve terminals within any individual muscle ( $t$  test;  $P < 0.01$ ), we limited our examination to 15 fortunate nerve terminals that had 12–47 consecutive active zones (mean = 24) exposed in a row. These 15 expansive views of individual nerve terminals, which we called our "series," were the basis of the anatomical data in Table I, which details the initial concentrations of 4-AP, the number of active zones found, and the overall level of activity, which varied from 0.9 to 15.2 vesicle openings/ $\mu\text{m}$  of active zone (mean = 5.7). Tracings of portions of six of these series are shown in Fig. 15.

If the activity at each active zone varied randomly within a particular series, then the overall activity in that series (percent of domains occupied by vesicle openings) could be used to determine the expected activity at each active zone, and this expected level could be compared with the actual values in a  $\chi^2$  test; 13 of the 15 series had randomly distributed activities by this test. Only two showed significant deviation ( $P < 0.01$ ) from the binomial distribution expected for randomness. These two series had relatively high levels of activity overall (32% of domains occupied by vesicle openings) but had large gaps of several active zones in a row where activity was very low. We concluded that such broad regional differences could result from variations in chilling before freezing, or other factors which could change the rate of vesicle collapse, and do not bear on the question of whether active zones interact with each other.

In the other 13 series, the variations in the level of activity were consistent with the idea that each active zone behaved independently of its neighbors. These series included all the terminals with low levels of activity and some with higher levels (up to 50% of the domains occupied by open vesicles). However, we were still concerned that even in these 13 "random" series, the level of activity might have varied gradually from one end of a nerve terminal to the other. Such an effect should have been detected by the tests just discussed, unless it was quite small. A more sensitive test was to examine each series of active zones for activity above and below the median. Thus, each

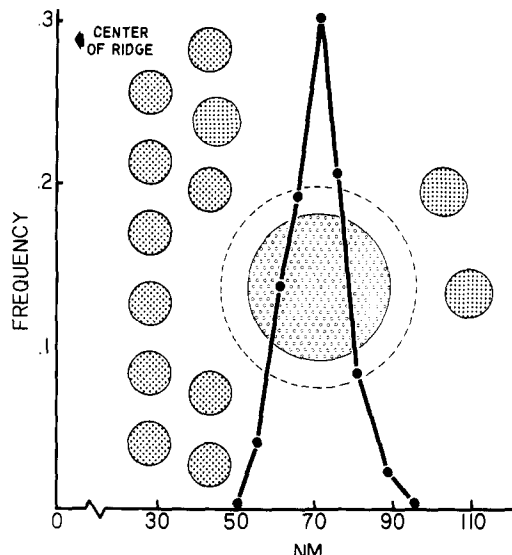


FIGURE 16 The frequency of observed vesicle openings expressed as a function of distance from the center of the active zone in frog nerve terminals. The graph represents 100 vesicle openings from three muscles stimulated once in 1 mM 4-AP, 4–5 ms before freezing. All dimensions are drawn to scale based on digitized measurements from freeze-fracture micrographs. This drawing thus represents an area like that boxed in Fig. 8. It illustrates the precise alignment of synaptic vesicle exocytosis to the presynaptic membrane specializations at the active zone. Obliquely stippled circles represent the large intramembrane particles which line up in two rows along both edges of the ridge which characterizes the active zone. A few even larger intramembrane particles, indicated by circles with horizontal stipple, are always found in the outer of the two rows, and in the immediate vicinity of the active zone. The large circle shaded with small circles represents the average diameter of the exocytotic openings these 100 synaptic vesicles formed with the plasma membrane, superimposed on the diameter of the underlying synaptic vesicle (dashed circle).

active zone was scored plus or minus according to whether its activity was greater or less than the median activity for the whole series. Then a run test was performed on the pluses and minuses, to look for regional variations within the series, by comparing the actual with expected number of runs. We found none; the mean of the deviations (in  $Z$  units) was  $-0.35$  and the individual values fell along a normal curve. Therefore, we could detect no tendency for the level of activity to vary along an individual nerve terminal. In general, then, the differences that we observed between

neighboring active zones in short segments of nerve terminals could be explained by random variation. Neighboring active zones appeared to become "turned on" to the same extent, as if they were all equally ready to discharge and were all equally affected by the arrival of the nerve impulse.

## DISCUSSION

The major goal of this work was to investigate the relationship between release of transmitter quanta and exocytosis of synaptic vesicles. We found that quick-freezing captured vesicle openings at the active zones on the nerve terminal membrane, just at the time quanta were released. If vesicle exocytosis were the mechanism of quantal transmitter release, there would be a correlation between the number of vesicles that open and the number of quanta released by a single stimulus. The orthodox form of the vesicle hypothesis (31) would predict one vesicle opening for each quantum released; and, in fact, our counts of vesicle openings over a wide range of transmitter release were consistent with this prediction (Fig. 14).

Our counts did not support the proposal that one quantum results from synchronous release of several vesicles. This alternative was proposed after recent high-gain recordings from vertebrate neuromuscular junctions revealed a class of MEPPs that were unusually small in amplitude (3, 35, 36, 55, 56). The proposal holds that "subminiature" EPPs represent the opening of individual synaptic vesicles, whereas normal full-sized MEPPs represent discharge of several vesicles simultaneously (35, 56). Contrary to this, our results indicated that, regardless of the level of transmitter release, the number of vesicle openings was not substantially greater than the number of quanta released. Of course, our estimates of total vesicle discharge and total quantal release per nerve terminal were both extrapolations from measurable data, and were subject to all the systematic errors presented in Section IV of Results. They could easily have been off by a factor of 2; that is, they could fit with the possibility that each normal-sized physiological quantum is generated by the exocytosis of two vesicles; but it would not likely be several vesicles.

Moreover, if several vesicles were released simultaneously, they would be expected to have some spatial association with each other. No such association could be seen in our pictures. Also, we

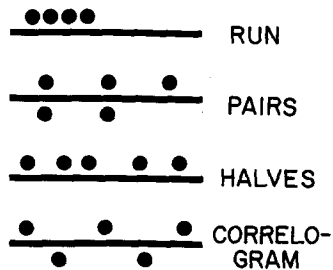


FIGURE 17 Diagram of the sorts of deviations from randomness tested for in analyzing the distribution of synaptic vesicle openings along the active zones of terminals frozen after stimulation in 4-AP.

used several statistical tests to look for hints of clustering and other nonrandom distributions of vesicle openings that might not be visually obvious. Still, the result at all levels of release was that the distribution of vesicle openings along individual active zones appeared random; that is, it could not be distinguished from a simple binomial process. Nor was there any indication that individual active zones on a particular terminal react in an all-or-none manner (56). In all but two of the series we studied, all of the release zones were equally active, within the limits of random variation. For the two series that were not, we will propose in a later paper that their variation was due to other factors, involving the rate of vesicle collapse after exocytosis. Thus, these statistical analyses indicate complete independence of each exocytotic event, and argue against the proposal that one quantum results from the synchronous release of several vesicles at an individual active zone. Instead, the complete randomness of vesicle openings indicates that the frog nerve terminal might just as well have one single active zone extending all along its length, instead of a series of short ones running transversely. Evolution must have selected transverse active zones at the frog endplate for some other reason than the control of transmitter release. Indeed, we could predict that the detailed geometry of how active zones are partitioned and arranged on different synapses depends on local tissue structure and does not reflect fundamental differences in the statistics of synaptic vesicle discharge.

In contrast to the random distribution of vesicle openings along the active zones, vesicle openings are spaced quite regularly with respect to the particle rows which line up at each individual active zone. Fig. 16 demonstrated that half of all

TABLE II  
*Tests for Distribution of Vesicle Openings at Individual Active Zones*

Test	No. of active zones*	Concn of 4-AP	M	Result	Probability
Run	100	$10^{-3}$		Deviations distributed normally	<0.01
Pair	50	$10^{-3}$		Deviations distributed normally	<0.01
Halves	50	$10^{-4}$		Deviations distributed normally	<0.01
Serial	50	$10^{-3}$		$r = 0$ up to five displacements	<0.01
Correlograms	50	$10^{-4}$			

Four tests for nonrandomness in vesicle exocytosis. The results of all four meant that the probability of a nonrandom process producing the observed distribution of vesicle openings was <0.01.

\* Each experimental group is from four muscles.

vesicles opened between 55 and 65 nm from the inner row of particles. This relationship suggests that the particles are somehow associated with exocytosis. One possibility, for example, is that they are rows of calcium channels (24, 27, 38). Consistent with this possibility, the morphological results illustrate that vesicles which approach these particles most closely have the best chance of release (cf. reference 24).

The massive transmitter output observed in 4-AP is not consistent with current estimates of the number of quanta immediately available for release, because it grossly exceeds these estimates. The estimates of pool size are based on evidence that the variability in quantal output is ordinarily very small and thus fits a binomial distribution (6, 43, 55). By applying binomial statistics, it is thus estimated that the size of the pool,  $n$ , is ~200–500. It has further been proposed that  $n$  represents the number of quanta, or vesicles, immediately available for release. However, since we could evoke release of at least 5,000 quanta and could visualize a similar number of vesicle openings after a single stimulus in 4-AP, it is apparent that the number of vesicles available for release must be considerably greater than 500.

One way that this unusual behavior of the nerve terminal in 4-AP could be reconciled with the binomial nature of release would be to argue that all of the many thousands of vesicles that are deployed along the active zones are somewhat

available for release, but that a few are much more likely to discharge than the others (2, 7). Differences in their propensity for discharge could result, for example, from a slight Brownian movement of vesicles and presynaptic calcium channels relative to each other. At normal levels of release, the factors initiating vesicle fusion would build up over such a short time that only the most probable of these vesicles would be released, so that  $n$  would be effectively very small. In 4-AP the release process is so much more intense and longer-lasting that vesicles with lower probabilities would also be recruited, but still only vesicles at the active zones. These active-zone vesicles are outnumbered by all the rest of the vesicles in the nerve terminal by at least 10:1 and, perhaps in some situations by as much as 100:1, so they are clearly in a preferential location for discharge. Whatever subtle factors might modulate their propensity to release and make certain vesicles at each active zone much more ready to go than their neighbors cannot so far be detected by these structural means.

In conclusion, the results presented here provide support for the proposal that during synaptic transmission the release of each quantum of transmitter is the result of exocytosis of one synaptic vesicle. Visualizing this rapid structural event by quick-freezing points up the general utility of this technique for the study of other rapid biological processes.

## APPENDIX 1

### Measurements

The method we developed for measuring freezing rates takes advantage of the fact that during freezing, the muscle is sandwiched between two conducting surfaces, the aluminum specimen mount above and the copper freezing block below. The muscle can then be treated as a dielectric between two conducting plates of a capacitor (Fig. 18). The value of this dielectric can be determined by applying a sinusoidal oscillating potential  $V$  to the aluminum specimen mount and measuring the transmission of current  $i$  through the muscle into

the copper freezing block. This gives a measure of the muscle capacitance  $C$  at any time after contact with the freezing block because:

$$i = \frac{V}{Z} \text{ and } Z = \frac{1}{j\omega C} \quad (1)$$

so,

$$C = \frac{i}{Vj\omega}, \quad (2)$$

where  $Z$  is the impedance (assuming an infinite resistance),  $j = \sqrt{-1}$ , and  $\omega$  is the frequency (100K Hz). This value of capacitance can be

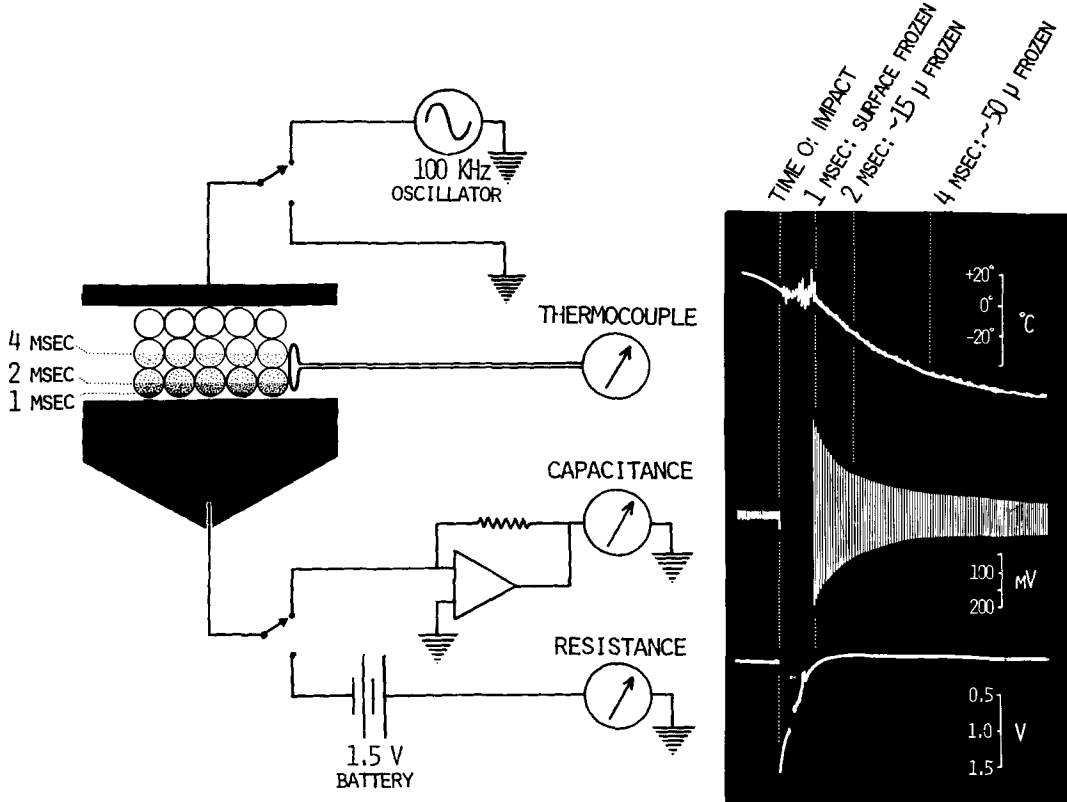


FIGURE 18 Diagram of the circuits used to measure the rate of freezing of the muscle. The muscle is shown schematically as the circles between the wedge-shaped copper freezing block below and the flat aluminum specimen mount above. The simplest circuit was a thermocouple placed in contact with the surface of the muscle; but no commercially available thermocouple was small enough to record what happened in the first 10–20  $\mu\text{m}$  where the freezing was best. Alternatively, a simple battery circuit was used to pass current through the muscle after contact with the copper block and thus to measure its resistance. As soon as a thin layer of ice formed on the muscle surface, the resistance became so high that this circuit was essentially broken. This happened in  $\sim 1$  ms. A better index was the change in muscle capacity during freezing, which was measured by applying a 100 Kz oscillating signal to the muscle mount and recording transmission through the muscle with a virtual-ground connected to the copper block. Once the surface had frozen and the relatively huge resistive current was over, the decline in capacitance was a measure of the subsequent growth of ice into the muscle, as explained in Appendix 1.

translated into a value for the tissue dielectric constant ( $\epsilon$ ) from:

$$C = \frac{\epsilon A}{d}, \quad (3)$$

where  $A$  is the area of the muscle and  $d$  is the distance between the aluminum and copper blocks, which is determined by the thickness of the plastic ring that prevents the muscle from being squashed.

At the initial moment of impact, before any freezing occurs, the muscle is filled with liquid water, which has a very high dielectric constant ( $\epsilon = 80$ ) because it is composed of polarized molecules that are free to orient in the imposed electric field. This dielectric value is not measured directly because the tissue fluid is an electrolyte, so a large resistive current flows between the aluminum and the copper upon impact. But  $<1$  ms later, this resistive current is cut off, presumably by the formation of a very thin layer of ice between the muscle and the copper block; so, from this time on, we can measure a pure capacitative current through the muscle, which declines progressively as the tissue freezes (Figs. 18 and 19).

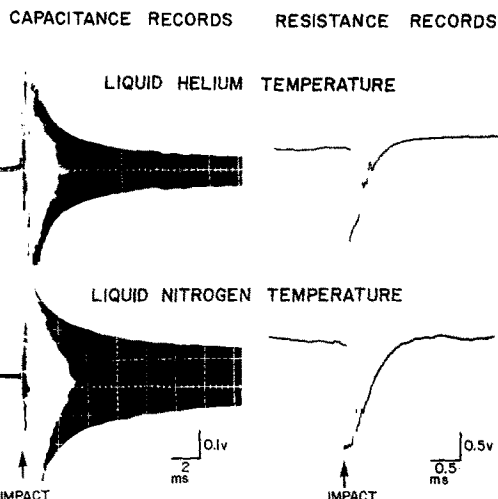


FIGURE 19 Representative oscilloscope traces of the change in capacitance and resistance of frog muscles during freezing by a copper block cooled to either  $4^\circ$  or  $77^\circ\text{K}$ . When the block starts at liquid helium temperature ( $4^\circ\text{K}$ ), a layer of ice stops the resistive current flow  $\sim 1$  ms after impact, and the capacitance falls halfway to its plateau in  $\sim 2$  ms. When the block is warmer, at liquid nitrogen temperature ( $77^\circ\text{K}$ ), the resistive current flow lasts  $\sim 1.5$  ms, and the capacitance declines to its halfpoint in  $\sim 4$  ms. Thus, a liquid nitrogen-cooled block is  $\sim 50$ - $100\%$  slower than a liquid helium-cooled one.

The current decreases as more and more of the tissue water turns into ice, presumably because ice, unlike water, has a very low dielectric constant ( $\epsilon = 2$ ) (54). In fact, if the ice front grows into the muscle as a plane parallel to the copper block, the tissue can be treated as two capacitors in series, one containing water and one containing ice. Initially, the ice capacitor is very thin; so even though it is filled with a medium of low dielectric constant, it has a high capacitance because  $d$  is small in Eq. 3. Thus, at first the total capacitance of the two layers is limited by the water-filled capacitor. As the thickness of the ice grows, the ice capacitor rapidly becomes the limiting one, and beyond  $5 \mu\text{m}$  thick dominates the two, despite the fact that the water capacitor is growing commensurately thinner. Assuming that:  $A = 1 \text{ cm}^2$ ,  $d_{\text{total}} = d_{\text{water}} + d_{\text{ice}} = 0.05 \text{ cm}$ ; and  $\epsilon_{\text{water}} = 80$  and  $\epsilon_{\text{ice}} = 2$  (cgs units), then, when the tissue is all water, the capacitance is  $140 \text{ pF}$ . When  $10 \mu\text{m}$  has frozen, the capacitance of the water phase has gone up only to  $142.5 \text{ pF}$ , but an ice capacitor of  $178 \text{ pF}$  has been added in series, giving a total capacitance ( $C_{\text{total}}$ ) of  $79 \text{ pF}$ , from

$$\frac{1}{C_{\text{total}}} = \frac{1}{178} + \frac{1}{142.5}.$$

When  $20 \mu\text{m}$  has frozen, the water phase has thinned a bit more and its capacitance has gone up to  $145 \text{ pF}$ , while the capacitance of the ice phase has dropped precipitously to  $89 \text{ pF}$  because it has doubled in thickness. Thus, the total capacitance is  $55 \text{ pF}$ , from

$$\frac{1}{C_{\text{total}}} = \frac{1}{145} + \frac{1}{89}.$$

Thus, assuming that ice grows into the tissue along a planar front, the change in capacitance should be dominated almost entirely by changes in the thickness of this planar ice layer and should be large enough to be measured easily.

In fact, the overall change in tissue capacitance that we observed in the first few milliseconds after impact was quite large (Fig. 19). We did not attempt to calculate muscle capacitances directly from this curve, because each muscle differed slightly in area and in thickness after impact. Instead, we calibrated this curve by inserting thin layers of plastic (Saran Wrap) between a series of test muscles and the copper block, when the block was warm; and then we measured the steady-state transmission of the oscillating signal through the

muscle. By adding progressively more and more layers of plastic, we generated a calibration curve relating the voltage of the signal transmitted to the thickness of the plastic insert, which matched the conditions during actual freezing experiments, and which could be used to translate voltages directly to thickness of ice simply by correcting for the difference between the dielectric constant of Saran Wrap ( $\epsilon = 3.4$ ) and that of ice ( $\epsilon = 2$ ).

Oscilloscope traces of the voltage transmitted through eight different muscles millisecond by millisecond during freezing gave the experimental curve for depth frozen vs. time shown in Fig. 21. It is most important to note that the region of the muscle up to 10–15  $\mu\text{m}$  deep, which is the only region that yields the well-frozen P-face views of nerves which are the basis of this paper, freezes in 2 ms or less.

### Theoretical

It is informative to compare this experimental freezing curve with the predicted rate of freezing derived from first principles concerning the diffusion of heat out of an extended body such as a muscle. This comparison should tell us whether there is still room for improvement in the freezing machine, or whether the machine has already approached the theoretical maximum rate of cooling.

Equations are available that predict how fast the heat will diffuse out of a solid warm body when the body is pressed against a planar surface that is kept at zero temperature (9). In simplest form, these equations predict that the temperature ( $v$ ) at distance  $X$  into the body at time  $t$  after initial contact with the cold block will be:

$$v = V \operatorname{erf} \frac{X}{\sqrt{4Dt}}, \quad (4)$$

where  $V$  is the initial temperature of the body and  $D$  is the diffusivity of heat within it.

Now, we do not know the temperature at which muscles actually freeze, but we can safely assume that it is necessary to remove enough heat to cool them from room temperature (+23°C) to 0°C, and, in addition, to remove all the heat released when ice is formed, which is 79.6 cal/g. This may be treated as equivalent to cooling the tissue 102.6°C, from +23°C to –79.6°C, even though it freezes before reaching –79.6°C, pausing at some warmer temperature until crystallization is complete. This assumption is the critical determinant

of the final values that will emerge from our theoretical treatment; it appears to be the same assumption used in an independent analysis of freezing velocity by Van Venrooij et al. (*Cryobiology*, 1975 **12**:46) which came to our attention after submitting our manuscript.

It would not be strictly correct to apply Eq. 4 simply by making  $V$  = room temperature (+297°K) and asking when  $v$  would reach the freezing temperature (297°–102.6°K), because the copper block is not exactly at 0°K to start with, and must warm up from 4°K when the muscle first strikes it. The assigned values of  $v$  and  $V$  should take account of this warm-up, if they are to reflect the true temperature gradients between metal and tissue before and after freezing.

We can calculate how much the copper block will warm up when the tissue hits it by using equations kindly provided by A. F. Huxley in June of 1976. These equations quantify what is intuitively obvious, namely, that the degree to which the surface of the copper will warm up depends on how fast it can absorb heat, relative to how fast the tissue can deliver heat to it. The rate of these heat fluxes will be determined by the temperature gradient between tissue and metal and by the thermal conductivity and thermal capacity of each of these materials. Huxley derived these equations by starting from the assumption that the temperature profile at any time ( $t$ ) in the metal and tissue would fit the curves in Fig. 20,

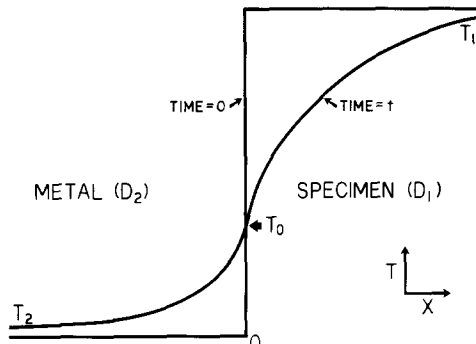


FIGURE 20 Diagram of the theoretical distribution of temperatures in metal freezing block and specimen just before (time = 0), and at any time after (time =  $t$ ), the two make contact. Huxley reasoned that, at the interface where the two make contact, the temperature at the surface of the metal block (which starts at  $T_2$ ) must very soon become the same as the temperature of the surface of the tissue (which starts at  $T_1$ ). This interface temperature may be called  $T_0$ . The other terms in this diagram correspond to those used in Eqs. 5 and 6.

which are described by,

for  $X > 0$ ; in the specimen:

$$\frac{T - T_0}{T_1 - T_0} = \frac{1}{\sqrt{\pi D_1 t}} \int_0^X e^{-\frac{X^2}{4D_1 t}} dX; \quad (5)$$

for  $X < 0$ ; in the metal:

$$\frac{T - T_0}{T_2 - T_0} = \frac{1}{\sqrt{\pi D_2 t}} \int_X^0 e^{-\frac{X^2}{4D_2 t}} dX, \quad (6)$$

where:

$$D = \text{heat diffusivity} = \frac{n}{p\sigma}, \quad (7)$$

when  $D$  = heat diffusivity,  $n$  = conductivity,  $p$  = density, and  $\sigma$  = specific heat (See Fig. 20 for explanation of other terms). It is  $T_0$ , the temperature at the interface between specimen and metal at equilibrium, that he wanted to know. To determine this, he assumed that, at equilibrium, heat flux out of the specimen would equal heat flux into the metal. Since heat flux equals  $n \frac{dT}{dX}$ , he could differentiate the above equations for each side of the interface:

$$n \frac{dT}{dX} = \frac{-n_1(T_1 - T_0)}{\sqrt{\pi D_1 t}} \quad (8)$$

(as  $X \rightarrow 0$  in specimen),

$$n \frac{dT}{dX} = \frac{-n_2(T_0 - T_2)}{\sqrt{\pi D_2 t}} \quad (9)$$

(as  $X \rightarrow 0$  in metal),

and set them equal, to obtain:

$$\frac{-n_1(T_1 - T_0)}{\sqrt{D_1}} = \frac{-n_2(T_0 - T_2)}{\sqrt{D_2}}. \quad (10)$$

Now, with Eq. 7, this can be rearranged to:

$$n_1 p_1 \sigma_1 (T_1 - T_0) = n_2 p_2 \sigma_2 (T_0 - T_2). \quad (11)$$

Then defining  $\sqrt{np\sigma} = A$  and rearranging gives the simple expression for  $T_0$ , the interface temperature:

$$T_0 = \frac{A_1 T_1 + A_2 T_2}{A_1 + A_2}. \quad (12)$$

Thus, the only influence of the metal on what happens inside the specimen is through the value of  $T_0$ , which is determined by the parameter  $A$ , a

measure of the thermal conductivity and heat capacity of the metal. In a previous publication (25), we erroneously stated that the rate of freezing would be determined by the thermal diffusivity of the metal, which is its thermal conductivity divided by its heat capacity, and we argued that copper would be a much better coolant at liquid helium temperature (4°K) than at liquid nitrogen temperature (77°K), because it has a much higher thermal diffusivity at the lower temperature. The following calculations of  $A$  show that this reasoning was not correct.

When the copper block is at liquid nitrogen temperature (77°K), its thermal conductivity is relatively low, only 1.42 cal/s·cm·°K; its density is 8.94 g/cm<sup>3</sup>; and its specific heat is relatively high,  $4.68 \times 10^{-2}$  cal/g·°K, so its  $A$  is 0.77.<sup>2</sup> In contrast, when the copper block is at 4°K, its thermal conductivity is very high, at 26.2 cal/s·cm·°K, and its density is still 8.94 g/cm<sup>3</sup>, but its specific heat is so very low, only  $2.15 \times 10^{-5}$  cal/g·°K, that its  $A$  is now only 0.071. We can see that with this low  $A$ -value the copper block would not be able to freeze the muscle without warming up considerably! This fact emerges directly from Eq. 12, once we calculate  $A$  for the ice in contact with the copper when equilibrium has been reached. Ice has a thermal conductivity four times higher than that of water,  $5.3 \times 10^{-3}$  cal/s·cm·°K, a density slightly less than water, 0.92 g/cm<sup>3</sup>, and a heat capacity half that of water, or 0.5 cal/g·°K, which gives  $A = 0.049$ . Assuming that  $T_1$  is room temperature (296°K), we can calculate  $T_0$  for a range of values of  $T_2$  (copper block temperature). The least warm-up ( $T_0 - T_2$ ) occurs when the copper block starts at 20°K. When the block is colder, its heat capacity and thus its  $A$  value is so low that Eq. 6 gives spuriously high values for  $T_0$ .

We conclude from these calculations that, in our actual experiments, when the block starts at 4°K, it warms soon after the tissue strikes it, to the lowest point in the  $T_0$  curve, 20°K, where its heat capacity is greater. The supposition that silver would be a better material for the freezing block because it has a higher thermal conductivity than copper at room temperature (51) does not hold up. At lower temperatures, silver is slightly less conductive than copper; and even though its density is slightly higher, its specific heat is only

<sup>2</sup> Units of  $A$  are cal/cm<sup>2</sup>·°K·s which are not directly informative and so are left out hereafter.

about half as great as copper, so its  $A$  value comes out only 0.67 over a broad range of temperatures from above 77°K to as low as 20°K.

Now we can return to Eq. 4 to determine the rate of cooling and say that the initial temperature  $V$  will be room temperature ( $273 + 23 = 296^{\circ}\text{K}$ ) minus the block temperature after warm-up ( $20^{\circ}\text{K}$ ), so  $V = 276^{\circ}\text{K}$ . The final temperature gradient at the moment that freezing is complete will be  $296^{\circ}\text{K} - 102.6^{\circ}\text{K}$  minus the block temperature  $20^{\circ}\text{K}$ , or  $v = 173.4^{\circ}\text{K}$ . Thus,  $v/V$  or the fraction of total cooling that has occurred at the time of freezing, will be  $173.4/276$  or  $\sim 0.6$ . We can see from a table of error functions that when  $\text{erf } X = 0.6$ ,  $X = 0.59$ ; so

$$\frac{X}{\sqrt{4Dt}} = 0.59.$$

Assuming that heat will be removed through water with diffusivity  $D = n/p\sigma$ , where conductivity ( $n$ ) =  $1.44 \times 10^{-3} \text{ cal/s} \cdot \text{cm} \cdot {}^{\circ}\text{K}$ , density ( $p$ ) =  $1.0 \text{ g/cm}^3$  and specific heat ( $\sigma$ ) =  $1.0 \text{ cal/g} \cdot {}^{\circ}\text{K}$ , its thermal diffusivity will be  $1.44 \times 10^{-3} \text{ cm}^2/\text{s}$  and so  $\sqrt{4D} = 0.076$ . Hence

$$\frac{X}{\sqrt{4Dt}} = \frac{X}{0.076\sqrt{t}} = 0.59$$

or  $\sqrt{t} = 22.33 X$ . This predicted relationship between depth ( $X$ ) and time taken to freeze ( $t$ ) is plotted for comparison with the actual values we obtained (Fig. 21). Note that the actual values roughly parallel the values predicted by Eq. 4, but are all  $\sim 0.5-1.0$  ms slower than expected. Possibly, this lag represents the time taken for the phase change from water to ice. Alternatively, it may simply reflect that the dielectric constant of ice does not reach its low point of 2 until the ice has reached  $-75^{\circ}\text{C}$ .

In a previous paper (25), we plotted the predicted rate of freezing assuming that heat would be removed through ice instead of through water, which fit the equation  $\sqrt{t} = 11.64 X$ . Since ice is four times more conductive than water, those predicted freezing rates were thus four times faster

than we have now measured. Given the many simplifications inherent in the calculations of freezing rates presented here, particularly the treatment of the heat of fusion of water as an equivalent amount of temperature change, and given the uncertainties about the thermal properties of ice and water at very low temperatures, it is impossible to know which theoretical curve should come closest to being correct. It is clear that the freezing technique used here approaches, but may still fall short of, the fastest cooling that could be achieved by heat transfer between two solids. In any case, it is clear that freezing with a copper block cooled only to liquid nitrogen temperature will be 50% slower than freezing with a block cooled all the way down to liquid helium temperature. This we have substantiated by recording significantly slower rates of capacitance change when frog muscles are applied to a copper block cooled only to  $77^{\circ}\text{K}$  rather than to  $4^{\circ}\text{K}$  (Fig. 19).

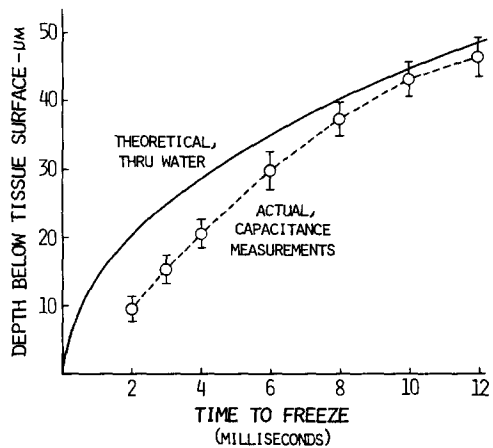


FIGURE 21 Comparison between the theoretical rate of freezing vs. depth curve calculated in Appendix 1, assuming that heat transferred through water, and the actual capacitance measurements obtained from eight frog muscles frozen against copper cooled to liquid helium temperature. Note that at a depth of  $\sim 10 \mu\text{m}$ , where ice crystal damage is minimal, freezing occurs in 2 ms or less. All the nerve terminals analyzed in this report were taken from such superficial regions.

## APPENDIX 2

A simple way of measuring the increase in acetylcholine release produced by 4-AP is to determine how much curare is needed to block the muscle twitch in each concentration of 4-AP. This was accomplished in the following manner: Four cutaneous pectoris nerve-muscle preparations were dissected from small frogs and bathed in the same concentration of 4-AP, and then each was exposed to a different dose of curare within the range expected to block the twitch in that concentration of 4-AP. For example, four muscles exposed to 1 mM 4-AP were bathed in 0.5, 0.75, 1.0, and  $2.5 \times 10^{-4}$  M curare. After 45 min in 4-AP and curare, each muscle was placed under a dissecting microscope, and one 5-V shock lasting 0.3 ms was applied to its nerve. In this way, the dose of curare barely sufficient to block twitch in all of the fibers of the muscle could be observed directly for each concentration of 4-AP without our needing to stimulate repeatedly and run the risk of fatiguing the preparation. As noted earlier, this fatigue is a consequence of the massive acetylcholine release produced by 4-AP (Fig. 9) and was particularly obvious in the four muscles exposed to 1 mM 4-AP. The muscles in 0.5 and  $0.75 \times 10^{-4}$  M curare twitched vigorously to the first shock but much more weakly to subsequent shocks. (A weaker twitch meant that a smaller number of fibers had EPPs that reached the threshold for spike initiation.) The muscle in  $10^{-4}$  M curare twitched vigorously only to the first shock, and only a few fibers within it twitched to the second shock. The muscle in  $2.5 \times 10^{-4}$  M curare did not twitch at all, not even to the first shock; thus, the EPPs in all of its fibers must have been subthreshold in this dose of curare.

For each level of 4-AP, this four-muscle procedure was repeated four times with different sets of muscles, to take account of variations from animal to animal. From this, we concluded that it took on the average  $2 \times 10^{-4}$  M curare to block the muscle twitch in 1 mM 4-AP. Column 3 of Table III displays the "critical" curarizing doses determined in this way at each level of 4-AP. Knowing these values and the  $K_D$  of curare at the endplate, we used the dose-ratio equation of Gaddum (23) to calculate the relative concentration of acetylcholine released into the cleft by a single stimulus in each dose of 4-AP (cf. reference 53):

$$\frac{[A']}{[A]} = \frac{[B]}{K_D} + 1. \quad (1)$$

TABLE III  
*Calculation of Quantal Content from Critical-Curarizing Dose of Curare*

(1) Calcium concn <i>mM</i>	(2) 4-AP concn <i>M</i>	(3) "Critical" curar- izing dose <i>M</i>	(4) Dose-ratio	(5) Calculated esti- mate of quantal content
2	0	$2.5 \times 10^{-6}$	1.8	100
10	0	$8.0 \times 10^{-6}$	3.75	180
10	$10^{-5}$	$3.0 \times 10^{-5}$	2.7	700
10	$10^{-4}$	$8.0 \times 10^{-5}$	2.5	1,900
10	$10^{-3}$	$2.0 \times 10^{-4}$		4,600

Average doses of curare needed to block the twitch of groups of four cutaneous pectoris muscles, different groups exposed to the five conditions listed in columns 1 and 2, and the resulting dose-ratio of curare obtained in going from one condition to the next. These data were used to estimate the quantal content in each level of 4-AP, as explained in the text.

This is the same equation that Jenkinson (30) used to determine the  $K_D$  of curare at the frog neuromuscular junction in the first place. The ratio of  $[A']$ , the concentration of agonist (acetylcholine) required to produce a given response (a barely subthreshold EPP) in the presence of a competitive antagonist (curare), versus  $[A]$ , the concentration of agonist required to produce the same response in the absence of the antagonist, is proportional to the concentration of the antagonist  $[B]$  divided by its dissociation constant  $K_D$ ; i.e., this ratio is a measure of the proportion of receptors made unavailable by the antagonist. The equation is derived from simple principles of mass action, and assumes only that (a) curare and acetylcholine compete one-for-one with the same receptor, which Jenkinson (30) has substantiated, and that (b) curare comes on and off the receptor fast enough so that it competes fairly with acetylcholine, even during the brief duration of the endplate current. Recent evidence indicates that curare dissociates from the receptor with a half-time of 0.5 ms, which is indeed well within the 3 ms rise time of the endplate current in 4-AP (1, 47). Therefore, the assumptions underlying this equation should be valid for our situation.

To compare two different doses of curare, the dose-ratio equation was rearranged by simple algebra to:

$$\frac{A''}{A'} = \frac{B'' + K_D}{B' + K_D}, \quad (2)$$

where one and two primes indicate the presence of different 4-AP concentrations. This equation was then used to calculate the dose-ratios in Column 4 of Table III. Neuromuscular junctions in the small muscles used in our experiments released only  $\sim 100$  quanta per impulse in Ringer's with the usual 2 mM concentration of calcium. This value was then multiplied by each succeeding dose-ratio to obtain the number of quanta per impulse at each level of 4-AP, displayed in Column 5 of Table III.

One difficulty in using this technique to estimate increases in acetylcholine release pertains to the calculated difference in output between 2 and 10 mM calcium. Raising calcium affects the muscle as well as the nerve in many different ways. Two of these effects would lead to an underestimate of the increase in acetylcholine release: (a) raising calcium increases muscle threshold (11), so the EPP in muscles paralyzed in 10 mM calcium must actually have been larger than in 2 mM calcium; and (b) raising calcium reduces the depolarizing action of acetylcholine on the endplate (21, 44), so even more acetylcholine must have been released to produce the larger EPP in 10 mM calcium. On the other hand, raising calcium also reduces the blocking action of curare, by increasing its  $K_D$  (30); so the added amount of curare needed just to overcome this effect would lead us to overestimate the increase in acetylcholine release in going from 2 to 10 mM calcium. Unfortunately, it was impossible to know how to balance these errors, so we chose not to use the curare dose-ratio at all for the transition between 2 and 10 mM calcium, and instead used a straightforward comparison of intracellularly recorded EPP's in a fixed dose of curare, before and after the increase in calcium. By this method, we obtained augmentations of 1.5- to 2.0-fold, so we used the value of 1.8-fold obtained the same way by del Castillo and Engbaek (14) and del Castillo and Stark (17) many years ago.

Special thanks to A. F. Huxley for providing the theoretical analysis of freezing rates described in Appendix 1; to Charles F. Stevens and Karen Pettigrew for providing guidance on the statistical tests; to Cliff Patlak and Herb D. Landahl for reviewing the statistical data and the math used in Appendix 1; to David Armstrong for outlining the quantitative basis of the dose-ratio test used in Appendix 2; to Frank McKeon for the tedious task of performing anatomical measurements; and to Trudy Nicolson for drawing Fig. 2.

Our heartiest thanks to Jim Wall, Senior Mechanician in the Department of Physiology, for his role in designing and building the freezing machine.

This work was supported by U. S. Public Health Service funds provided through the National Institute of Neurological Disorders and Stroke, intramural to T. S. Reese and extramural to J. E. Heuser and M. J. Dennis; and also by generous research grants from the Muscular Dystrophy Association of America (MDAA).

During this work, L. Jan was an NIH Postdoctoral Fellow and Y. Jan was an MDAA Postdoctoral Fellow. Our heartiest thanks to Jim Wall, Senior Mechanician in the Department of Physiology, for his role in designing and building the freezing machine.

*Received for publication 28 June 1978, and in revised form 19 December 1978.*

## REFERENCES

- ARMSTRONG, D., and H. A. LESTER. 1977. Kinetics of curare action at the frog nerve-muscle synapse. *Neuroscience*, **3**:369. (Abstr.).
- BARTON, S. B., and I. S. COHEN. 1977. Are transmitter release statistics meaningful? *Nature (Lond.)*, **268**:267-268.
- BEVAN, S. 1976. Sub-minature end-plate potentials at untreated frog neuromuscular junctions. *J. Physiol. (Lond.)*, **258**:145-155.
- BIRKS, R. I. 1973. The relationship of transmitter release and storage to fine structure in a sympathetic ganglion. *J. Neurocytol.*, **3**:133-160.
- BIRKS, R., H. E. HUXLEY, and B. KATZ. 1960. The fine structure of the neuromuscular junction of the frog. *J. Physiol. (Lond.)*, **150**:134-144.
- BRANISTEANU, D. D., M. D. MIYAMOTO, and R. L. VOLLE. 1976. Effects of physiologic alterations on binomial transmitter release at magnesium depressed neuromuscular junctions. *J. Physiol. (Lond.)*, **254**:19-37.
- BROWN, T. H., D. H. PERKEL, and M. W. FELDMAN. 1976. Evoked neurotransmitter release: Statistical effects of nonuniformity and non-stationarity. *Proc. Natl. Acad. Sci. (U. S. A.)*, **73**:2913-2917.
- BULLIVANT, S. 1965. Freeze substitution and supporting techniques. *Lab. Invest.*, **14**:1178-1189.
- CARSLAW, H. S., and J. C. JAEGER. 1947. *Conduction of Heat in Solids*. Clarendon Press, Oxford.
- CECCARELLI, B., W. P. HURLBUT, and A. MAURO. 1973. Turnover of transmitter and synaptic vesicles at the frog neuromuscular junction. *J. Cell Biol.*, **57**:499-524.
- CONSTANTIN, L. L. 1968. The effect of calcium on contraction and conductance thresholds in frog skeletal muscle. *J. Physiol. (Lond.)*, **195**:119-132.
- COUTEAUX, R., and M. PECOT-DECHAVASSINE. 1970. Vesicules synaptiques et poches au niveau des "zones actives" de la jonction neuromusculaire. *C. R. Acad. Sci. Ser. D*, **271**:2346-2349.
- COUTEAUX, R., and M. PECOT-DECHAVASSINE. 1974. Les zones spécialisées des membranes presynaptique. *C. R. Acad. Sci. Ser. D*, **280**:299-301.
- DEL CASTILLO, J., and L. ENGBAEK. 1954. The nature of the neuromuscular block produced by magnesium. *J. Physiol. (Lond.)*, **124**:370-384.
- DEL CASTILLO, J., and B. KATZ. 1954. Statistical factors involved in neuromuscular facilitation and depression. *J. Physiol. (Lond.)*, **124**:574-585.
- DEL CASTILLO, J., and B. KATZ. 1955. Local activity at a depolarized nerve-muscle junction. *J. Physiol. (Lond.)*, **128**:396-411.
- DEL CASTILLO, J., and L. STARK. 1952. The effect of calcium ions on the motor end-plate potentials. *J. Physiol. (Lond.)*, **116**:507-515.
- DEMSEY, G. P., and S. BULLIVANT. 1976. A copper block method for freezing non-cryoprotected tissues to produce ice-crystal-free regions for electron microscopy. *J. Microsc. (Oxf.)*, **106**:251-270.
- DUNANT, Y., J. GAUTRON, M. ISRAËL, B. LESBATS, and R. MANARANCHE. 1974. Changes in acetylcholine level and electrophysiological response during continuous stimulation of the electric organ of *Torpedo marmorata*. *J. Neurochem.*, **26**:635-643.
- ERÄNKÖ, O. 1954. Quenching of tissues for freeze-drying. *Acta Anat.*, **22**:331-335.
- FATT, P., and B. KATZ. 1952. Spontaneous subthreshold activity at

- motor nerve endings. *J. Physiol. (Lond.)*, **117**:109-128.
22. FRANKENHAUSER, B. 1957. The effect of calcium on the myelinated nerve fiber. *J. Physiol. (Lond.)*, **137**:245-260.
  23. GADDUM, J. H., K. A. HAMUD, D. E. HATHWAY, and F. F. STEVENS. 1955. Quantitative studies of antagonists for 5-hydroxytryptamine. *Quart. J. Exp. Physiol. Cogn. Med. Sci.* **40**:49-74.
  24. HEUSER, J. E. 1976. Morphology of synaptic vesicle discharge and reformation at the frog neuromuscular junction. In *Motor Innervation of Muscle*. S. Thesleff, editor. Academic Press, London, 51-115.
  25. HEUSER, J. E. 1977. Synaptic vesicle exocytosis revealed in quick-frozen frog neuromuscular junctions treated with 4-aminopyridine and given a single electrical shock. In *Neuroscience Symposia*. Vol 2. W. M. Cowan, and J. A. Ferrendelli, editors. Society for Neuroscience, Bethesda, Md. 215-239.
  26. HEUSER, J. E., and T. S. REESE. 1973. Evidence for recycling of synaptic vesicle membrane during transmitter release at the frog neuromuscular junction. *J. Cell Biol.* **57**:315-344.
  27. HEUSER, J. E., T. S. REESE, and D. M. D. LANDIS. 1974. Functional changes in frog neuromuscular junctions studied with freeze-fracture. *J. Neurocytol.* **3**:109-131.
  28. HEUSER, J. E., T. S. REESE, and D. M. D. LANDIS. 1976. Preservation of synaptic structure by rapid freezing. *Cold Spring Harbor Symp. Quant. Biol.* **40**:17-24.
  29. JAN, Y. N., L. Y. JAN, and M. J. DENNIS. 1977. Two mutations of synaptic transmission in *Drosophila*. *Proc. R. Soc. Lond. B. Biol. Sci.* **198**:87-108.
  30. JENKINSON, D. H. 1960. The antagonism between tubocurarine and substances which depolarize the motor end-plate. *J. Physiol. (Lond.)*, **152**:309-324.
  31. KATZ, B. 1969. *The Release of Neural Transmitter Substances*. Liverpool University Press, Liverpool, England.
  32. KATZ, B., and R. MILEDI. 1965. The measurement of synaptic delay, and the time course of acetylcholine release at the neuromuscular junction. *Proc. R. Soc. Lond. B. Biol. Sci.* **161**:483-495.
  33. KATZ, B., and R. MILEDI. 1965. Propagation of electric activity in motor nerve terminals. *Proc. R. Soc. Lond. B. Biol. Sci.* **161**:453-482.
  34. KATZ, B., and R. MILEDI. 1967. A study of synaptic transmission in the absence of nerve impulses. *J. Physiol. (Lond.)*, **192**:407-436.
  35. KRIEBEL, M. E., and C. E. GROSS. 1974. Multimodal distribution of frog miniature endplate potentials in adult, denervated and tadpole leg muscle. *J. Gen. Physiol.* **64**:85-103.
  36. KRIEBEL, M. E., F. LLADOS, and D. R. MATTESEN. 1976. Spontaneous subminiature endplate potentials in mouse diaphragm muscle: evidence for synchronous release. *J. Physiol. (Lond.)*, **262**:553-581.
  37. LETINSKY, M. S., K. H. FISCHBECK, and U. J. McMAHAN. 1976. Precision of reinnervation of original postsynaptic sites in frog muscle after a nerve crush. *J. Neurocytol.* **5**:691-718.
  38. LINAS, R. R., and J. E. HEUSER. 1977. Depolarization-release coupling systems in neurons. *Neurosci. Res. Program Bull.* **15**:No. 4.
  39. MANALIS, R. S. 1977. Voltage-dependent effect of curare at the frog neuromuscular junction. *Nature (Lond.)*, **267**:366-367.
  40. MARCHBANKS, R. M., and M. ISRAËL. 1972. The heterogeneity of bound acetylcholine and synaptic vesicles. *Biochem. J.* **129**:1049-1061.
  41. MARTIN, A. R. 1955. A further study of the statistical composition of the end-plate potential. *J. Physiol. (Lond.)*, **130**:114-122.
  42. MARTY, A., T. NEILD, and P. ASCHER. 1976. Voltage sensitivity of acetylcholine currents in *Aplysia* neurons in the presence of curare. *Nature (Lond.)*, **261**:501-503.
  43. MIYAMOTO, M. D. 1975. Binomial analysis of quantal transmitter release at glycerol treated frog neuromuscular junctions. *J. Physiol. (Lond.)*, **250**:121-142.
  44. NASTUK, W. C., and J. H. LIU. 1966. Muscle postjunctional membrane: changes in chemosensitivity produced by calcium. *Science (Wash. D. C.)* **154**:266-267.
  45. PFENNINGER, K., K. AKERT, H. MOOR, and C. SANDRI. 1971. Freeze-fracturing of presynaptic membranes in the central nervous system. *Philos. Trans. R. Soc. Lond. B. Biol. Sci.* **261**:387-389.
  46. PFENNINGER, K., K. AKERT, H. MOOR, and C. SANDRI. 1972. The fine structure of freeze-fractured presynaptic membranes. *J. Neurocytol.* **1**:129-149.
  47. SHERIDAN, R. E., and H. A. LESTER. 1977. Rates and equilibria at the acetylcholine receptor of *Electrophorus* electroplaques. A study of neurally evoked postsynaptic currents and of voltage-jump relaxations. *J. Gen. Physiol.* **70**:187-219.
  48. SNEDECOR, G. W., and W. G. COCHRAN. 1967. *Statistical Methods*. Iowa State University Press. 6th edition.
  49. SOKAL, R. R., and F. J. ROHLF. 1969. *Biometry*. W. H. Freeman, San Francisco, California.
  50. TAKEUCHI, A., and N. TAKEUCHI. 1960. On the permeability of end-plate membrane during the action of transmitter. *J. Physiol. (Lond.)*, **154**:52-67.
  51. VAN HARREVELD, A., and J. CROWELL. 1964. Electron microscopy after rapid freezing on a metal surface and substitution fixation. *Anat. Rec.* **149**:381-386.
  52. VAN HARREVELD, A., J. TRUBATCH, and J. STEINER. 1974. Rapid freezing and electron microscopy for the arrest of physiological processes. *J. Microsc. (Oxf.)*, **100**:189-198.
  53. WAUD, D. R. 1968. Pharmacological receptors. *Pharmacol. Rev.* **20**: 49-87.
  54. WEAST, R. C., editor. 1977. *Handbook of Chemistry and Physics*. CRC Press, Cleveland, Ohio. 58th edition.
  55. WERNIG, A. 1975. Estimates of statistical release parameters from crayfish and frog neuromuscular junction. *J. Physiol. (Lond.)*, **244**: 207-221.
  56. WERNIG, A., and H. STIRNER. 1977. Quantum amplitude distributions point to functioned unity of the synaptic 'active zone'. *Nature (Lond.)*, **269**:820-822.
  57. WHITTAKER, V. P. 1965. The application of subcellular fractionation techniques to the study of brain function. *Prog. Biophys. Mol. Biol.* **15**:39-96.
  58. WHITTAKER, V. P., W. B. ESSMAN, and G. H. C. DOWE. 1972. The isolation of pure cholinergic synaptic vesicles from the electric organs of Elasmobranch fish of the family *Torpedinidae*. *Biochem. J.* **128**:833-846.
  59. YEH, J. Z., G. S. OXFORD, C. H. WU, and T. NARAHASHI. 1976. Dynamics of aminopyridine block of potassium channels in squid axon membrane. *J. Gen. Physiol.* **68**:519-535.
  60. ZIMMERMAN, H., and M. J. DOWDALL. 1977. Vesicular storage and release of a false cholinergic transmitter (acetylpyrrolcholine) in the *Torpedo* electric organ. *Neuroscience*, **2**:731-739.
  61. ZIMMERMAN, H., and V. P. WHITTAKER. 1974. Effect of electrical stimulation on the yield and composition of synaptic vesicles from the cholinergic synapses of the electric organ of *Torpedo*: a combined biochemical, electrophysiological and morphological study. *J. Neurochem.* **22**:435-450.